

Evaluating the Performance of Transfer Function Models for Identifying Groundwater Disturbances in Infrastructure Projects

Master's Thesis in Infrastructure and Environmental Engineering

Viktor Alfredsson
Ella Blomquist

DEPARTMENT OF ARCHITECTURE AND CIVIL ENGINEERING

Chalmers University of Technology
Gothenburg, Sweden 2025
www.chalmers.se

MASTER THESIS 2025

Evaluating the Performance of Transfer Function Models for Identifying Groundwater Disturbances in Infrastructure Projects

Viktor Alfredsson
Ella Blomquist



CHALMERS
UNIVERSITY OF TECHNOLOGY

Department of Architecture and Civil Engineering
CHALMERS UNIVERSITY OF TECHNOLOGY
Gothenburg, Sweden 2025

Evaluating the Performance of Transfer Function Models for Identifying Groundwater Disturbances in Infrastructure Projects

Viktor Alfredsson

Ella Blomquist

© VIKTOR ALFREDSSON, ELLA BLOMQUIST, 2025.

Supervisor: Ezra Haaf, Architecture and Civil Engineering, Chalmers University of Technology

Supervisor: Daniel Erdal, Tyréns

Supervisor: Johanna Larsson, Tyréns

Examiner: Lars Rosén, Architecture and Civil Engineering, Chalmers University of Technology

Degree project report 2025

Department of Architecture and Civil Engineering

Chalmers University of Technology

SE-412 96 Gothenburg

Sweden

Telephone +46 31 772 1000

Cover: Plotted graph of the groundwater head time series with multiple potential stress scenarios occurring. The scenarios indicate implementations of synthetic shafts made in the benchmark model.

Typeset in L^AT_EX

Gothenburg, Sweden 2025

Evaluating the Performance of Transfer Function Models for Identifying Groundwater Disturbances in Infrastructural Projects

Predicting Groundwater levels at Haga Station construction site in Västlänken Project

VIKTOR ALFREDSSON, ELLA BLOMQUIST

Department of Architecture and Civil Engineering

Chalmers University of Technology

Abstract

Hydrogeology is inherently challenged by the difficulty of making direct observations. To address this, numerical groundwater models are commonly developed to simulate hydrogeological conditions at specific study sites. However, such models require extensive input data and are often time- and resource-intensive. As a result, alternative, data-driven modeling techniques are of growing interest.

This study evaluates the performance of a data-driven Transfer Function model in identifying and analyzing groundwater head disturbances caused by underground excavation activities. The transfer function model used for this project is the open-source Python package Pastas. Focusing on the Haga Station site within the Västlänken infrastructure project in Gothenburg, Sweden, the research compares transfer function models with a numerical benchmark model developed using MODFLOW. Synthetic and constructed disturbance scenarios in the form of excavation shafts were modeled in the benchmark model to generate time series of groundwater head, leakage and infiltration. These time series were then used to test the transfer function model's ability to detect controlled disturbances. To validate the results, a qualitative assessment was also performed using observed field data.

The findings demonstrate that transfer function models developed using Pastas can replicate general groundwater trends and detect some disturbance signals. However, the models showed significant variation between different well simulations, with inconsistencies in how disturbances were interpreted. Additional limitations include the overestimation of recharge and the underestimation of leakage into shafts following transfer function model calibration. Despite these challenges, the transfer function approach shows promise due to its low data requirements and its ability to model complex hydrogeologic study sites. This work contributes to a better understanding of transfer function model capabilities and their potential application in hydrogeological assessments of infrastructure projects.

Keywords: Transfer function models, Time series analysis, Data-driven modeling, Pastas, MODFLOW, Groundwater Head Disruptions, Underground Infrastructure Project, Residuals.

Acknowledgements

This master's thesis was conducted during the spring semester of 2025 at Chalmers University of Technology by Viktor Alfredsson and Ella Blomquist. The project marks the conclusion of the master's program in Infrastructure and Environmental Engineering at the Department of Architecture and Civil Engineering.

The idea for this study was introduced to us by our supervisor, Ezra Haaf, researcher at the Division of Geology and Geotechnics at Chalmers. We would like to express our gratitude to Ezra for proposing this interesting topic and for providing guidance and support throughout the project. We also extend our thanks to Sofie Axéen, doctoral student at the same division, for her guidance on numerical modeling techniques.

Furthermore, we would like to thank Daniel Erdal and Johanna Larsson at Tyréns for their assistance with providing relevant data and for offering constructive feedback during the thesis work. Finally, we wish to thank Anna Albersson and Jonas Lissdaniels from Trafikverket for arranging an insightful site visit to the tunnels of the Västlänken project.

Viktor Alfredsson and Ella Blomquist, Gothenburg, June 2025

List of Acronyms

Below is the list of acronyms that have been used throughout this thesis listed in alphabetical order:

FEFLOW	Finite-element modeling program for simulating groundwater flow
GUI	Graphical user interface for pre- and post-processing MODFLOW
GWF	Groundwater Flow
GWH	Groundwater Head
HFB	Horizontal Flow Barrier
HOB	Head Observation
INF	Infiltration
MNW2	Multi Node Well package 2
MODFLOW	Modular three-dimensional finite-difference ground-water flow model
PET	Potential evapotranspiration
SGU	Swedish Geological Investigation (Sveriges Geologiska Undersökning)
SMHI	Swedish Meteorological and Hydrological Institute
TFN	Transfer Function Model
TMO	The Swedish Transport Administration's measurement database for environmental impact (Trafikverkets mätdatabas för omgivningspåverkan)
WTF	Water Table Function

Contents

List of Acronyms	ix
List of Figures	xiii
List of Tables	xv
1 Introduction	1
1.1 Aim	2
1.2 Research questions	2
1.3 Limitations	3
2 Data and Methods	5
2.1 Modeling workflow	5
2.2 Study site	6
2.2.1 Haga Station	6
2.2.2 Hydrogeological conditions	6
2.2.3 Observation wells and time series	9
2.2.4 Climate data	10
2.3 Benchmark modeling	12
2.3.1 Site-based numerical groundwater flow model	13
2.3.2 Synthetic benchmark model	15
2.3.3 Synthetic shafts and event time line	16
2.4 Data driven modeling using Pastas	20
2.4.1 Response functions	20
2.4.2 Time series modeling process	20
2.4.3 Evaluation of time series fit	21
2.5 Model evaluation	21
2.5.1 Synthetic scenario data	21
2.5.2 Observational time series	22
2.5.3 Benchmark time series	22
2.5.4 Scenarios with synthetic shafts	23
3 Results and Discussion	25
3.1 Calibration of benchmark model	25
3.2 Observational time series	26
3.3 Scenarios with synthetic shafts	28
3.3.1 Plotted transfer function models with all synthetic shafts	28

3.3.2	Identification of impact of synthetic shafts	29
3.4	Implications for transfer function analysis of perturbed time series . .	33
3.5	Outlook	35
4	Conclusion	37
	References	39
A	Plotted graphs	I
A.1	Evapotranspiration	I
B	Appendix: Python code	III
B.1	Eto	III
B.2	Appendix: Recharge and plotting	V
B.3	Appendix: Python code for measured values	VI
B.4	Appendix: Python code for benchmark generated time series	IX
C	Pastas models plotted graphs	XIII
C.1	Pastas, measured values	XIII
C.2	Appendix: Pastas models, simulated values with constructed distur- bances	XVI
C.2.1	Estimated groundwater head with constructed disturbances .	XVII
C.3	Appendix: Pastas models, simulated values with synthetic distur- bances from A, B and C shaft	XVIII

List of Figures

2.1	Flowchart illustrating the structure and integration of input time series used in the modeling process.	6
2.2	Profile view of the planned traverse of Västlänken with soil and bedrock layer (Trafikverket, 2020).	7
2.3	Overview of the study site and its groundwater flow directions (Sundkvist and Wallroth, 2016).	8
2.4	Map of the location of the wells. The Handels shaft is in the center with faint marking of fictional shafts and the tunnel. Wells, infiltration well (INF) and the Handels shaft are labeled.	10
2.5	The amount of recharge (m/day) over time.	12
2.6	Map of the benchmark model domain, bordered in black. Located in the Haga area in Gothenburg.	14
2.7	An overview of the study area with the Handels shaft and the fictional shafts, marked as A, B and C in the figure. The purple and red line consists of the railway tunnel.	18
2.8	Timeline of the benchmark model with extended time for calibration of TFM. The single letters and numbers indicates when each shaft layer is incorporated into the model.	19
2.9	Graph of the observed leakage over time.	22
2.10	Graph of the groundwater leakage into modeled shafts from the benchmark model with logarithmic scale. Including the Handels shaft and shaft A, B and C.	23
3.1	Groundwater flow out from the MODFLOW model caused by DRN package during one week, starting 2022-09-08, in model row 71 in m^3/s . Plotted in ModelMuse through the model layers and cells, represented in black.	26
3.2	TFM simulation based on measured values for borehole HH4117U.	27
3.3	Situation map of the TFM simulated borehole HH4117U together with the Handels shaft and infiltration well.	28
3.4	TFM simulation based on benchmark generated values for HH4117U with fictional disturbances of A,B & C shafts.	29
3.5	Residuals from TFM simulations with different scenarios for HH4117U.	30
3.6	Difference in residuals from the scenarios compared to the base scenario for HH4117U. Values are taken from the benchmark model.	30
3.7	Residuals from TFM simulations with different scenarios for HH4266U.	31

3.8	Difference in residuals from the scenarios compared to the base scenario for HH4266U. Values are taken from the benchmark model.	31
3.9	Situation map of the TFM simulated borehole HH7453U together with the Handels shaft, infiltration well and synthetic shafts.	32
3.10	Residuals from TFM simulation with different scenarios for HH7453U.	32
3.11	Difference in residuals from the scenarios compared to the base scenario for HH7453U. Values are taken from the benchmark model.	33
3.12	TFM simulation with limited calibration based on simulated values for HH4117U.	34
3.13	TFM simulation with limited calibration based on simulated values for HH4266U.	34
A.1	The amount of PET (m/day) over time.	I
C.1	Pastas simulation based on measured values for HH4266U.	XIII
C.2	Pastas simulation based on measured values for HH7453U.	XIV
C.3	Pastas simulation based on measured values for HH7455U.	XV
C.4	Pastas simulation based on simulated values for HH4266U.	XVI
C.5	Pastas simulation based on simulated values for HH7453U.	XVII
C.6	Pastas simulation with limited calibration based on simulated values for HH7453U.	XVIII
C.7	Pastas simulation with limited calibration based on simulated values for HH7455U.	XVIII
C.8	Pastas simulation with shaft A, B and C on simulated values for HH7453U.	XIX
C.9	Pastas simulation with shaft A, B and C on simulated values for HH7455U.	XX

List of Tables

2.1	Details about measurement of groundwater head at observation wells. Missing values of wells HH4279B and HH7453U.	10
2.2	Table of all tested scenarios for the synthetic shafts A, B and C.	24

1

Introduction

Groundwater plays a vital role in maintaining ecological balance, providing drinking water, and supporting industrial and agricultural activities (Condon et al., 2021). However, human activities such as urbanization, construction, and resource extraction can significantly alter groundwater conditions, leading to potential environmental and engineering challenges.

Common environmental and engineering challenges are tunneling and underground excavation projects. A primary concern is groundwater leakage, where excavation may create pathways for water intrusion, resulting in lowered groundwater levels. This drop in the water table can reduce pore pressure, potentially causing ground subsidence and structural instability (Wikby et al., 2024; Panda and Vipulanandan, 2019; Omoko et al., 2018). Given the inherent complexity of hydrogeological systems, comprehensive analysis is critical for understanding groundwater behavior and mitigating associated risks.

Particularly in urban areas, groundwater modeling plays a crucial role in quantifying and integrating available data, improving predictions, and supporting decision making in hydrogeological studies (Anderson et al., 2015).

Groundwater models can range from simple to complex, depending on the problem, but its methods and assumptions must be evaluated to ensure that they are appropriate and produces scientifically defensible results (Reilly and Harbaugh, 2004). Numerical process-based models such as MODFLOW and FEFLOW are widely used in hydrogeological studies due to their ability to simulate complex groundwater systems (Sun et al., 2022). However, in complex hydrogeological areas, such models typically require a lot of field data to conduct a reliable model, which raises the demand for more cost- and time-effective modeling options.

Data-driven groundwater models mainly analyze historical data and the relationship between groundwater level and other significant factors such as groundwater recharge and groundwater withdrawal (Haaf et al., 2023; Collenteur et al., 2024). Unlike numerical models, data-driven models do not attempt to replicate physical processes and solve three-dimensional groundwater-flow equations but instead focus on empirical relationships. Data-driven models have been shown to be helpful in simplifying complex physical hydrogeological systems, and this study is specifically focused on data-driven transfer function models in urban areas (Vonk et al., 2024; Lindblom and Boström, 2021).

Transfer function model is a modeling method that is used to transform input data in the form of a time series into an output result (Collenteur et al., 2021). One modeling tool to utilize transfer function models is Pastas, which is code-based and built using Python scripts. The advantage of using transfer function modeling tools such as transfer function model is the low number of parameters needed to calibrate the model (Bakker & Schaars, 2019). According to Collenteur et al. (2021), the transfer function modeling tool, Pastas, is frequently used together with developing a numerical model. Using a code-centered tool provides more transparency in the modeling process than a numerical modeling tool with a graphical user interface (GUI), as the user can see all inputs and is often required to perform all calculations manually.

1.1 Aim

The aim of this study is to evaluate the capability of a data-driven transfer function model to identify and analyze groundwater head disturbances caused by infrastructure excavation, modeled in a synthetic benchmark model. By using data-driven, transfer function models (TFM) to simulate time series of groundwater head, the study investigates whether such models can detect changes in groundwater levels associated with specific subsurface activities, such as shaft construction. The project also aims to assess whether TFMs can complement, or in some cases, replace numerical groundwater flow models in hydrogeological analysis. A data-driven approach may offer a more cost-effective, time-efficient, and less complex alternative for modeling groundwater leakage in infrastructure projects.

1.2 Research questions

This study focuses on evaluating the effectiveness of data-driven transfer function modeling in detecting and interpreting groundwater disturbances caused by infrastructure excavation. The research questions below aim to explore the capabilities of the transfer function model compared to traditional process-based models and its potential as a practical tool in groundwater assessments for infrastructure projects:

- To what extent can transfer function models distinguish between groundwater disturbances caused by different disturbances, such as those caused by deep excavations?
- How accurately can transfer function models attribute each groundwater disturbance to its source?
- What are the limiting factors for evaluating groundwater disturbances with transfer function models.

1.3 Limitations

This study is limited to evaluating the ability of transfer function models to analyze and identify disturbances in the groundwater head. The analysis focuses specifically on transfer function models developed with TFMs at the Haga station site with a MODFLOW model as a benchmark model.

2

Data and Methods

2.1 Modeling workflow

To assess the capability of a transfer function model (TFM) to identifying and evaluating groundwater disturbances, multiple TFMs are developed using input data generated by a numerical model of the Haga area in Gothenburg. This numerical model serves as a benchmark framework, simulating various scenarios where all details of the system are known. Its primary function is to generate time series data for groundwater head, leakage into the modeled shafts, and infiltration flows from wells integrated into the system. These generated time series for different leakage scenarios, along with recharge data in Section 2.2.4, are used as input stresses for the TFMs.

The shafts in the benchmark model are based on the observed values of groundwater head, leakage, and infiltration provided by the Swedish Transport Administration (Trafikverket) ensuring a realistic representation of site conditions. The data sources are presented in Section 2.2.3. The same observed values are used to qualitatively validate the numerical model as a benchmark model, by simulating the observed values in a TFM and comparing the results to ensure the validity of the results. A flowchart illustrating the structure and integration of input time series used in the models is presented in Figure 2.1.

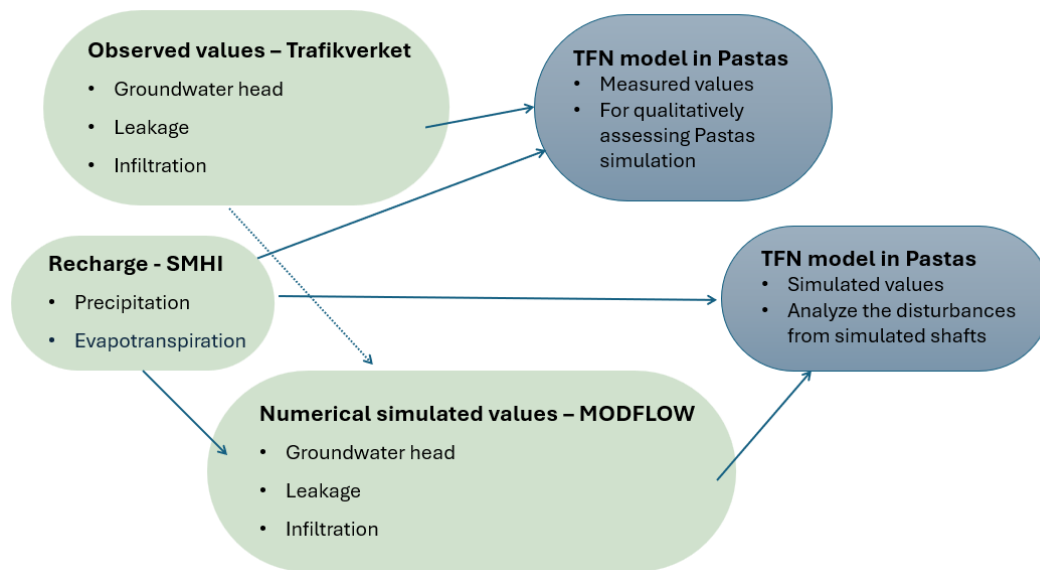


Figure 2.1: Flowchart illustrating the structure and integration of input time series used in the modeling process.

2.2 Study site

The selected study area is the Haga district in Gothenburg, which includes the Haga Station section of the Västlänken project and its surroundings. The Haga area was chosen due to its comprehensive and well-documented hydrogeological data, including groundwater head measurements from wells, as well as infiltration and leakage measurements.

2.2.1 Haga Station

The Västlänken project involves an 8 km double-track railway through central Göteborg, with approximately 6.6 km in tunnels excavated through rock and clay (Sundkvist and Wallroth, 2016). It includes three underground stations at Gothenburg Central, Haga, and Korsvägen. Construction began in 2018 and is expected to finish by 2030 (Trafikverket, 2021). One of the three entrances to the underground train platform will be at the School of Business, Economics and Law at the University of Gothenburg, locally referred to as "Handels". Therefore, the shaft that is constructed for this entrance is called the Handels shafts and will be the central disturbance and the reference point for other fictional disturbances modeled for this study.

2.2.2 Hydrogeological conditions

Sweden's bedrock primarily consists of ancient Precambrian crystalline rocks that form part of the Baltic Shield. The oldest formations are over 2.5 billion years old

(SGU, 2020). Most of these rocks formed during the Svecokarelian orogeny (2,000–1,650 million years ago), while the southwestern region of Sweden was later shaped by the Sveconorwegian orogeny.

The ground topography in Gothenburg is characterized by low-lying, soil-covered areas along the *Göta* River (north) and *Mölnålsån* (east), while the southern parts feature hilly terrain with elevated bedrock areas intersected by narrow, soil-filled valleys (Sundkvist and Wallroth, 2016). In the southern highlands, bedrock is exposed at the surface, whereas in the lowlands near rivers and valleys, it is overlain by thick clay deposits. The general soil profile consists of surface fill overlying soft clay, under which a friction soil layer rests on bedrock. Figure 2.2 shows a profile view of the soil layers along the Västlänken tunnel route.

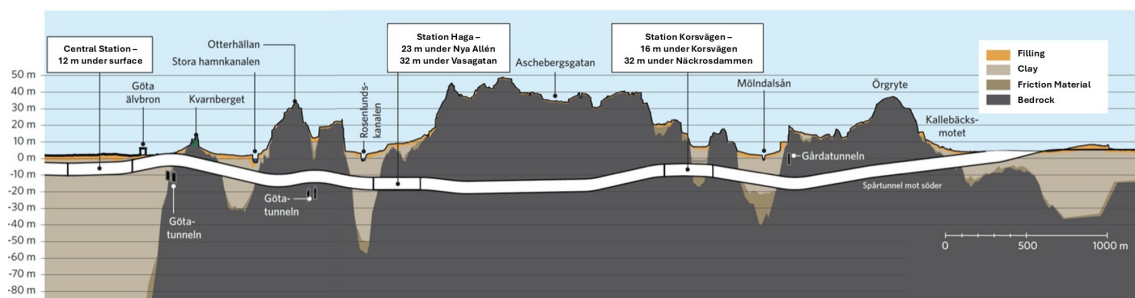


Figure 2.2: Profile view of the planned traverse of Västlänken with soil and bedrock layer (Trafikverket, 2020).

The site area is naturally divided hydrogeologically into a northern section, including Haga, and a southern section, including Annedal (Sundkvist and Wallroth, 2016). In the northern part, thick soil layers are bordered by high rock formations to the south. Within this area, there are two hydraulically interconnected lower groundwater reservoirs in the soil: the Masthugget–Haga reservoir in the north and the Olivedal–Annedal reservoir in the south. These reservoirs consist of frictional soil layers positioned above the bedrock. Bedrock levels within the Haga site vary significantly, with elevations ranging from approximately +60 m in higher areas to -60 m northwest of Skansberget, representing a total variation of at least 120 m. Figure 2.3 shows an overview of the study site and its groundwater flow directions.



Figure 2.3: Overview of the study site and its groundwater flow directions (Sundkvist and Wallroth, 2016).

Groundwater levels in the rock are influenced by existing draining rock structures, leading to locally disturbed conditions (Sundkvist and Wallroth, 2016). Measurements from rock boreholes indicate groundwater levels between +15 m and +21 m. Hydraulic conductivity values in the rock, based on core borehole testing, range from 2×10^{-9} to 1×10^{-7} m/s. The West Link route in this area passes through an area with high thickness of soil deposits, including Stora Hamnkanalen and Rosenlundskanalen. The Haga area is also prone to subsidence in areas with soft clay if groundwater drawdown occurs (Wikby et al., 2024). This subsidence poses a significant risk to the value, functionality, and structural stability of buildings within the drawdown zone, which can extend several hundred meters from the construction site. In some cases, permanent protective infiltration may be necessary to prevent

the impact of underground constructions on the built environment.

2.2.3 Observation wells and time series

The benchmark model and transfer function model (TFM) is calibrated on groundwater head from wells. The information used is time series, which describes the groundwater head over time. Infrequent observations of the groundwater head have been made, beginning from year 2000 for a few number of wells. Higher frequency of data points starts in 2018 for the remaining wells.

The observed head is collected from the well data given by Trafikverket's measurement database for environmental impact (TMO). Observed data includes measured data from wells taking active measurements during the ongoing construction. The observation also encompasses measurement of flow of water leaking into the Handels shaft and flow of water from the infiltration well. The input data are given in time series with a variation of time sequences from before construction start to finished project.

A section of wells is used to represent the groundwater heads in the study area. The selection is based on choosing wells distributed at varying distances from the shaft. This is to create a good overall picture of the entire area. Boreholes with a large amount of data points were prioritized to provide reliable data. The location of the wells can be seen in Figure 2.4 and Table 2.1. Wells closer to the shaft may be more affected by leakage disturbances. The coordinates for the wells are taken from Trafikverket with estimation made for the shaft where the coordinates for the closest wells is used to assess the location. Several wells are used for the transfer function model for analysis purposes to get a broad view of the infliction of the stresses on the groundwater in the area.



Figure 2.4: Map of the location of the wells. The Handels shaft is in the center with faint marking of fictional shafts and the tunnel. Wells, infiltration well (INF) and the Handels shaft are labeled.

Well label	Depth (m)	Diameter (cm)	Aquifer placement
HH4001H	35	11.5	Bedrock
HH4003H	52	11.5	Bedrock
HH4107U	15	5.1	Lower soil layer
HH4117U	16	5.1	Lower soil layer
HH4226U	2	5.0	Upper soil layer
HH4302U	28	5.1	Lower soil layer
HH7454U	14	6.3	Lower soil layer
HH7455U	6	6.3	Lower soil layer

Table 2.1: Details about measurement of groundwater head at observation wells. Missing values of wells HH4279B and HH7453U.

2.2.4 Climate data

External influences on the fluctuating groundwater level, caused by environmental factors, include primarily recharge. It describes the amount of rainwater that can

effectively add to the groundwater, with a reservation on the amount that can be evaporated. Recharge, R is calculated by the equation (2.1)(Collenteur et al., 2019), as follows.

$$R(t) = P(t) - E(t) \quad (2.1)$$

- R - Recharge
- E - Evapotranspiration
- P - Precipitation
- t - time

The input data is based on observations at the station Göteborg A (Gothenburg A) for all climate parameters except for solar radians, R_s , which is gathered from the station Göteborg Sol (Gothenburg Sun). Values are provided by Swedish Meteorological and Hydrological Institute (SMHI)(SMHI, 2025). Both weather stations are located in the center of the city and are chosen due to its high continuous measurement frequency and long timespan. The data are collected as time series with the daily mean value per day during the time period January 1, 2000 and November 30, 2024.

To estimate Evapotranspiration, the data undergoes processing to enhance consistency and comparability. For instance, relative humidity, R_h and solar radiance, R_s are given in hourly measurements and compressed into daily mean values. Solar radiance (Mj/m^2) is gathered from multiplying radiation (W/m^2) with the amount of sun time [s] and altered from how it is given from the source SMHI, to fit the needed units for later. See Appendix B.1 for further explanation of modifications made.

For calculations of recharge, the parameter evapotranspiration needed is done using the open-source Python package ETo is employed to determine the Potential Evapotranspiration (PET). Meteorological data is utilized in the FAO Penman-Monteith equation (Allen et al., 1998). The Python code used to calculate potential evapotranspiration (ETo) is provided in Appendix B.1.

To make the PET calculation feasible, additional parameters such as the mean saturation vapour pressure, e_s and the actual vapour pressure, e_a must be defined. To calculate this, the saturated vapor pressure e_0 is required and depends on temperature, as shown in equation (2.2). The actual vapor pressure, e_a is used in PET calculations as an average over one day which is defined needing the mean saturation vapour pressure, e_s . This is defined using maximum and minimum temperature with the saturated vapour pressure in equation (2.3) (Allen et al., 1998). The air's relative humidity, RH is a ratio between e_a and e_s , which can be converted to equation (2.4) and used to conclude the needed parameter for further Pet calculations in the Python package Eto (see Appendix B.1).

$$e^0(T) = 0.6108 * e^{\frac{17.27 * T}{T + 237.3}} \quad (2.2)$$

$$e_s = \frac{e^0(T_{\max}) + e^0(T_{\min})}{2} \quad (2.3)$$

$$e_a = \frac{R_h * e_s}{100} \quad (2.4)$$

- e^0 - saturation vapour pressure (kP)
- e_s - mean saturation vapour pressure (kPa)
- e_a - Actual water vapour pressure (kPa)
- R_h - Relative humidity (-)
- T - Temperature (Celsius)

The amount of evapotranspiration that totals during one day can be seen in Figure A.1 in the Appendix A.1.

Calculations contribute to the input data used for the simulation of the benchmark model and the TFM. Figure 2.5 shows the calculated daily amount of recharge (m) with the start date of January 1, 2000. The recharge is calculated by subtracting the evapotranspiration from the precipitation by the equation 2.1, which results in negative recharge during periods of very little precipitation. The data points are changed to weakly mean the total amount of recharge over one day, as elaborated in Appendix B.2.

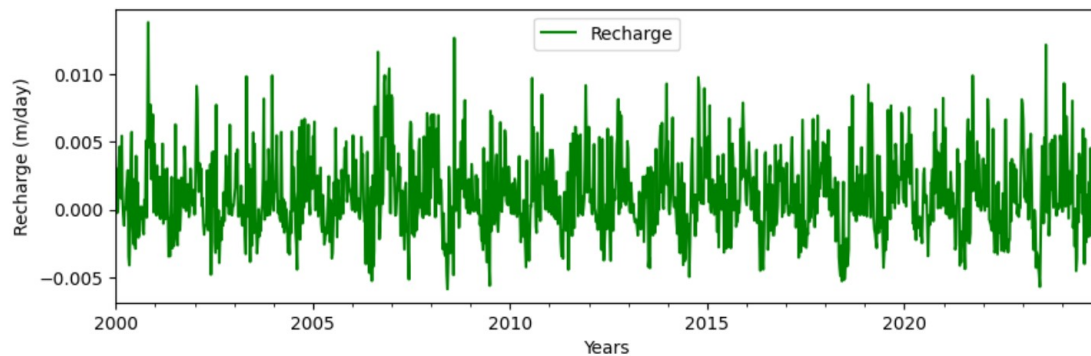


Figure 2.5: The amount of recharge (m/day) over time.

2.3 Benchmark modeling

MODFLOW is a modular finite-difference groundwater flow modeling software developed by the United States Geological Survey (USGS) (Harbaugh, 2005). It simulates the movement of groundwater through aquifers by solving the groundwater flow equation in three dimensions. MODFLOW is free to use and is widely regarded as the international standard for simulating and predicting groundwater and surface

water systems (USGS, 2022). There exist several versions of MODFLOW, this study uses MODFLOW-NWT because of its flexibility in adjusting model parameters and rewetting implementations (Niswonger et al., 2011).

Initial configuration of MODFLOW models requires defining geometry, initial groundwater head, soil properties, e.g. hydraulic conductivity (Winston, 2023). In addition to these factors, external properties that influence and define groundwater head and flow must also be considered. Once relevant data have been collected, the model can be subjected to disturbances caused by load, such as tunneling and excavation (Winston, 2023). For this work, the ModelMuse GUI was used for pre- and post-processing MODFLOW.

2.3.1 Site-based numerical groundwater flow model

The base numerical model used as benchmark for this project was developed using MODFLOW-NWT. The initial aim of this model was to study the importance of explicitly representing measurements of hydraulic head from open boreholes in crystalline rocks (Haaf et al., 2025). The same model was also modified to analyze groundwater leakage into the Västlänken tunnel (Lilja and Zander, 2024). While based on the same hydrogeological data and climate data, the later model represents three years of data, 2020 to 2023, divided into two 18-month periods before and after tunnel construction, to assess and quantify leakage.

The benchmark model covers the Haga area in central Gothenburg, including parts of the Port of Gothenburg, with a particular focus on the planned location of the Haga Station for Västlänken, as shown in Figure 2.6 below. It is discretized into 18 numerical layers representing coarse-grained fill, underlain by a layer of clay and coarse-grained fill, followed by the bedrock which is further divide into 14 separate layers (Haaf et al., 2025).

The initial model had MODFLOW time steps set to one-week intervals to manage computational complexity for the two 18-month periods (Lilja and Zander, 2024). One-week intervals are also used to analyze disturbances in this project, but over an extended period of six years. The validated model has been calibrated using observed groundwater head data from five wells, employing the Multi-Node Well (MNW2) package and Head Observation (HOB) package in MODFLOW (Haaf et al., 2025). Additionally, it incorporates the recharge (RCH) package to simulate precipitation during the study period with data from SMHI, accounting for natural infiltration processes described in Section 2.2.4. To represent stormwater management in the area, the Drain (DRN) package is included to drain excess water from the top layer.

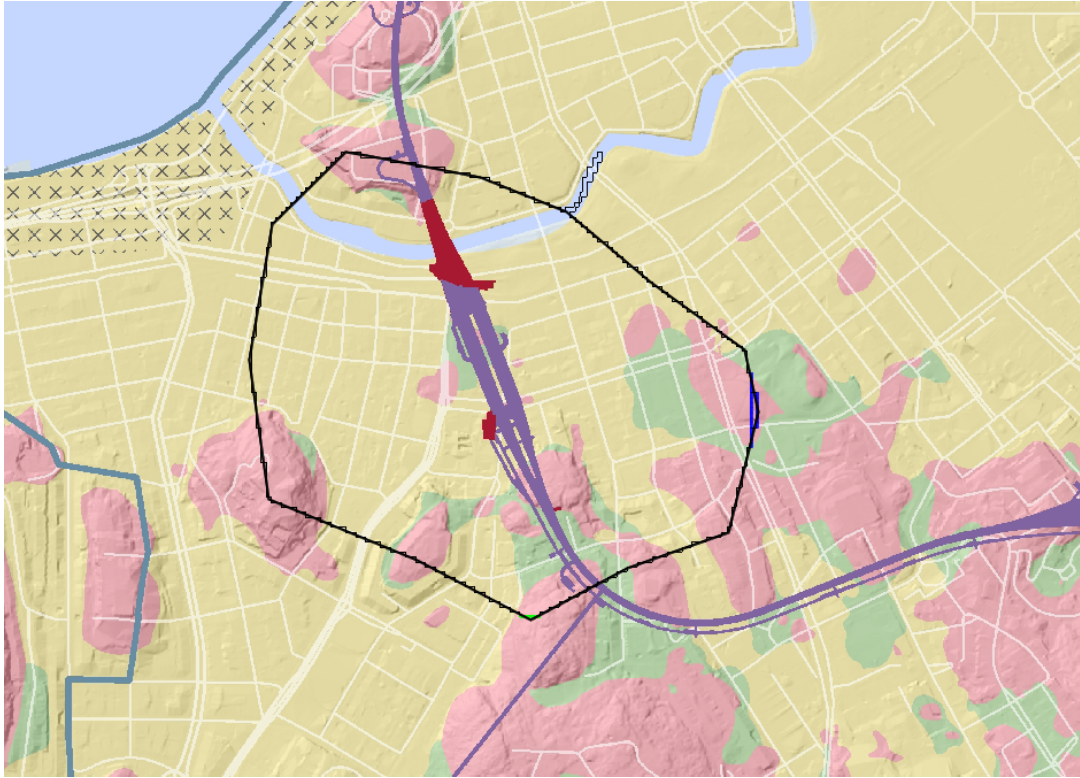


Figure 2.6: Map of the benchmark model domain, bordered in black. Located in the Haga area in Gothenburg.

2.3.2 Synthetic benchmark model

The objective of recalibrating the initial numerical model and add additional disturbances is to generate different time series that will be used as an input to the TFM. Because the aim of the study includes testing the accuracy of transfer function models to identify different disturbances, multiple different model versions must be modeled with different sets of disturbances.

The disturbances incorporated into the model is in the form of various shafts, except the previously modeled Västlänken tunnel, which is modeled as a one-dimensional drain. Since the goal is to analyze potential disturbances and test TFMs to identify and quantify their effects against a benchmark, not all modeled shafts need to exist or be planned in reality. However, their impact on the system must be realistically represented to reflect potential future infrastructure projects.

To establish a reference case, the Handels shaft is modeled first, which is a completed shaft with fixed dimensions. This shaft is selected because several boreholes surrounding it have provided continuous groundwater level measurements before, during, and after construction. Instead of modeling the shaft with detailed input to estimate the future potential impact, the shaft is modeled to reflect the observed impacts that have been measured. These observed groundwater levels from nearby boreholes as well as the leakage data provided by Trafikverket, serve as a baseline, allowing direct comparison with the simulated results. By aligning the model output with real-world data, the accuracy and reliability of the simulation in representing groundwater responses to shaft construction is improved.

Several approaches are available for modeling a shaft in MODFLOW, and the optimal method depends on the specific objectives of the model and the physical processes being represented. One commonly used and computationally simple method involves representing the shaft as a zone of high vertical hydraulic conductivity. In this approach, the shaft is modeled as a vertical column of cells with significantly elevated vertical conductance values, which facilitates a rapid downward movement of water from the surface to the bottom of the shaft zone. This setup allows water entering the shaft through horizontal inflow or precipitation to quickly move downward through the model layers.

In the case of the Handels shaft, water that infiltrates into a shaft is captured and removed through pumping systems and drainage infrastructure. With the high-conductivity method, water remains within the model, just migrating downward rather than being extracted. To better represent actual conditions, the MODFLOW Drain (DRN) package was utilized instead. The DRN package allows for the specification of a zone or boundary condition where water is removed from the model once the groundwater head exceeds a defined elevation. This functionality mimics the physical process of pumping or draining water from the shaft, effectively removing it from the modeled system.

To quantify the volume of water removed via the DRN package within the shaft

region, the Zone Budget package was utilized. This package enables the definition of custom zones within the model, allowing detailed water balance calculations for specific areas, in this case, the zone surrounding the shaft. Once a zone is defined and the model is run, the Zone Budget package generates output files that report the volumes of water entering and exiting the zone at each time step. These outputs are broken down by flow components, including those associated with the Drain package. As a result, it is possible to isolate and extract the volume of water removed through the drains at each time step, which is one of the necessary inputs to the TFM to assess its capability.

The Drain (DRN) package in MODFLOW allows the user to specify drain conductance, either per unit length or area, which directs the rate at which water is removed from the model area. This conductance value is a parameter that typically must be calibrated empirically if the objective is to simulate the shaft for predictive purposes for hydrogeological scenarios. In the case of the Handels shaft, however, the volume of water leakage into the shaft is already known from measurements, provided by Trafikverket (Hagman et al., 2024). This prior knowledge enables a more targeted calibration approach. Rather than beginning with arbitrary conductance values, the conductance was set to equal the horizontal hydraulic conductivity (K_x) of each model cell intersected by the shaft.

The neutral conductance for the DRN package was kept as the horizontal hydraulic conductivity and instead the shaft walls and bottom were modeled separately to more accurately represent the structure of the Handels shaft. The shaft walls are built of 1-meter-thick concrete, reinforced with corrugated steel frames, and the bottom of the shaft lies against bedrock that has been sealed through concrete injection. The bottom of the shaft was modeled with low hydraulic conductivity cells to simulate the concrete injected bedrock while the shaft walls were represented using the Horizontal Flow Barrier (HFB) package with a thickness of one meter.

In conjunction with the construction of the Handels shaft, three infiltration wells are installed to mitigate drawdown effects caused by the excavation by pumping water into the ground. (Hagman et al., 2024). These wells are designed to infiltrate water to a specified level using a tilt mechanism, controlling the flow of water according to the current groundwater level (Hagman et al., 2024). Therefore, these wells were modeled using the Multi-Node Well Package 2 (MNW2), which is a head-dependent flux boundary that also enables positive infiltration rates depending on the current groundwater head at the well location (Niswonger et al., 2011). The resulting infiltration rates for the benchmark model is presented in section 3.1.

2.3.3 Synthetic shafts and event time line

To assess the transfer function model's capability to identify groundwater disturbances, three synthetic shafts, named A, B, and C, are incorporated into the numerical benchmark model developed in MODFLOW. These synthetic shafts are equal

in their geometry and assigned identical hydraulic properties to those of the existing Handels shaft. However, each shaft is extended vertically down to the bedrock interface and therefore differs in total depth due to the varied thickness of the overlying soil layers. Each shaft is introduced in three successive vertical segments, with a temporal lag of two weeks between the addition of each segment. This stepwise approach is intended to reflect realistic construction dynamics and enable temporal resolution of the model's response to incremental disturbance. The shafts are positioned at different locations across the model area to capture a range of hydraulic responses from different observation wells, see Figure 2.7. By distributing the synthetic shafts at varying distances from the boreholes used as observation points, the model enabled the monitoring of resulting drawdown patterns. This setup is designed to evaluate the performance of the transfer function model in detecting temporally distributed disturbances to the groundwater system in the area.

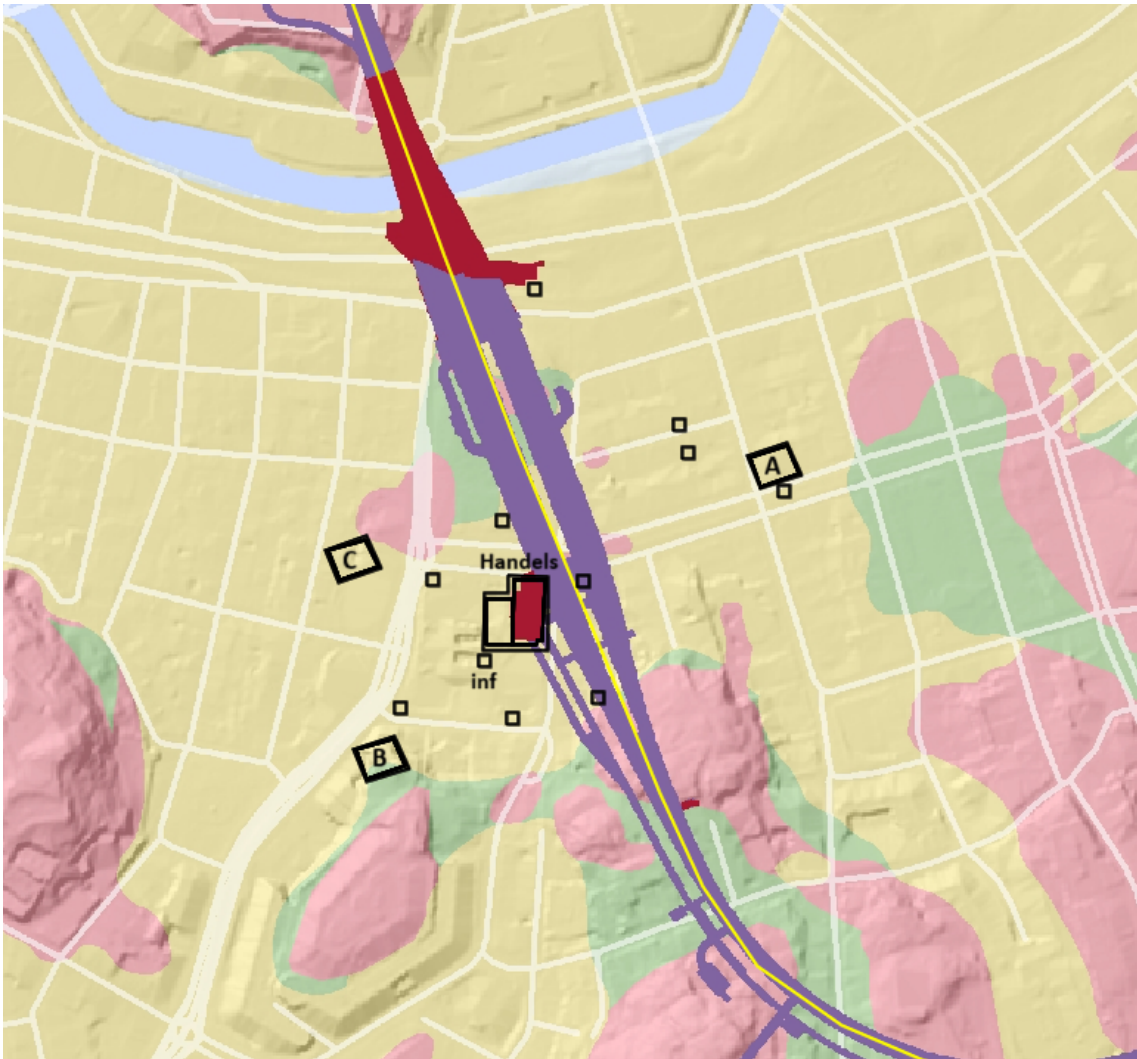


Figure 2.7: An overview of the study area with the Handels shaft and the fictional shafts, marked as A, B and C in the figure. The purple and red line consists of the railway tunnel.

The original model was designed to cover a three-year period, from October 1, 2020, to September 30, 2023 (Lilja and Zander, 2024). However, to achieve an effective step response and a realistic model fit, the transfer function model required a longer calibration period before it could accurately analyze and detect disturbances. Therefore, the time span of the numerical model was extended to cover the period from September 28, 2017, to November 28, 2024, providing more than enough time for proper calibration for the TFM. This change was made by extending the recharge data calculated in Section 2.2.4 with the measured data from SMHI, and incorporating it into the RCH package in MODFLOW. Figure 2.8 shows a timeline of the MODFLOW-NWT model, visualizing when each major component is incorporated into the model.

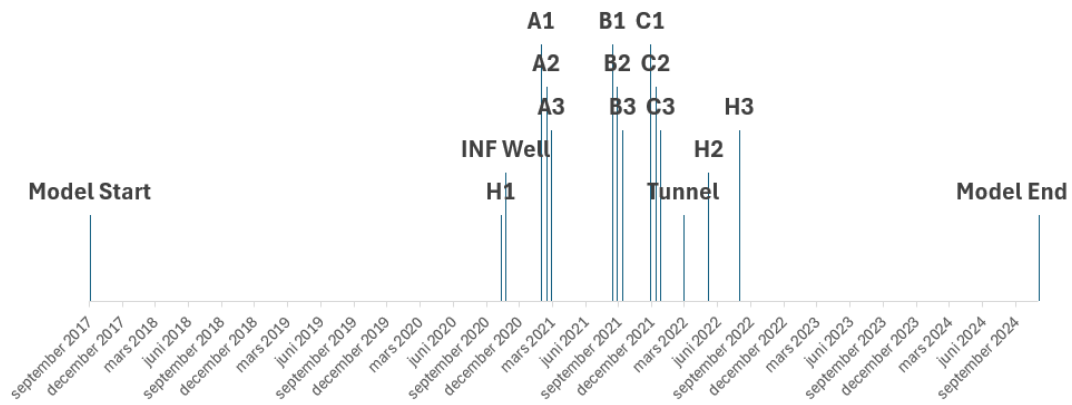


Figure 2.8: Timeline of the benchmark model with extended time for calibration of TFM. The single letters and numbers indicates when each shaft layer is incorporated into the model.

2.4 Data driven modeling using Pastas

TFMs are used to predict the groundwater head using time series of groundwater head from observed values to calibrate the it. The Modeling method is object-oriented, meaning that simulations are made on singular observation wells. Individual models are made for each observation well that is analyzed and repeated for every additional observation well. Time series refers to the observed groundwater level measured in a specific well over time (Collenteur et al., 2019). Stresses are added to the model to replicate real-life disturbances that effects the groundwater table.

2.4.1 Response functions

The groundwater head, $h(t)$ is calculated on the base elevation, d , meaning the initial groundwater head in a base scenario without disturbances (Collenteur et al., 2019). The sum of inflict on the groundwater head that all of the disturbances sources have, results in the theoretical groundwater head. The initial elevation is used with the impact of groundwater change to predict and calculate the affected head.

$$h(t) = \sum_{m=1}^M h_m(t) + d + r(t) \quad (2.5)$$

- $h(t)$ - observed groundwater head.
- $h_m(t)$ - head contribution from stresses
- m - stresses
- d - initial elevation
- $r(t)$ - residuals

The disturbances are used in the calculation based on their contributions, meaning their effect on the height difference in the groundwater level. A response function is used to transform the stresses into appropriate stress models (Collenteur et al., 2019).

2.4.2 Time series modeling process

Individual TFMs are developed for each well to initiate the time-series analysis. The influence of external stresses on groundwater head is represented using the following two stress models. Recharge was incorporated through the *RechargeModel*, which simulates the effects of precipitation and evapotranspiration (Collenteur et al., 2019). Leakage and infiltration were represented using the *WellModel*, which accounts for the distance between the stress source and the observation well (Collenteur et al.,

2019). The stress models are then applied to each model and simulated as a response function.

2.4.3 Evaluation of time series fit

To the coefficient of determination, R^2 is used to evaluate the reliability of the simulation made in the TFM. The value of R^2 ranges between 0 and 1, with 1 being a result with strong correlation and 0 meaning that there is no correlation to input data (Onyutha, 2022). A R^2 value greater than 0.5 verifies that the simulated value can prove its authenticity by comparing them to external time series. It is important to note that the coefficient of determination does not quantify the bias of the simulation (Onyutha, 2022). For the current project, an R^2 value around 0.8 and higher is desired to ensure accurate modeling results.

2.5 Model evaluation

A parallel modeling workflow has been applied for applying the TFM. The first sets of models are calibrated using observed values, while the second are calibrated using values from a benchmark model. In the first approach, observed data are used in the modeling simulation to evaluate its ability to replicate the actual impact of the excavation of the shaft, as measured in nearby wells. The second approach, introduces synthetic shafts to test whether the transfer function model can detect and quantify the disturbances they cause. These synthetic shafts are created in the benchmark model and subsequently used as time series input to calibrate the transfer function model.

2.5.1 Synthetic scenario data

Simulation of TFMs with synthetic benchmark input data is done with the base scenario, meaning when only the Handels shaft is built and then when the synthetic shafts are implemented. It is important to note that shaft A, B and C are represented as leakage when added to the TFMs. However, the shafts existence affects the simulation in its entirety, ergo also the time series with groundwater level and infiltration. Therefore, benchmark data of groundwater head, leakage, and infiltration are extracted in two separate versions, one with only the Handels shaft and one with all of them. Consistent input data is needed to allow the contracts of the simulation to reflect correctly in the results.

The groundwater head is used to calibrate and validate the model with further simulation where the TFM's calibration on the groundwater head is limited to a certain time. The TFM predicts the groundwater head on its own accord for the remaining simulation sequence. Time series from the benchmark model is used to validate the simulation done in TFMs to analyze its usability of the simulation method.

2.5.2 Observational time series

To qualitatively assess the reliability of the numerical benchmark model, multiple TFMs were simulated using observed field data, based on measured groundwater head, recharge, leakage, and infiltration. The purpose of this assessment is to highlight the limitations of the benchmark model as a base for modeling disturbance scenarios in TFMs. When running the models, a selection of the borehole results in more accurate time series simulations of groundwater head than others.

The model uses time series of groundwater levels, construction leakage, and infiltration as input. To assess the TFM's ability to simulate real conditions, it is run using actual well data. The results are then compared to observed groundwater drawdowns to evaluate the correlation. Extended explanation on how can be seen in the Python code in Appendix B.3

The observed leakage caused by the construction of the Handels shaft is shown in Figure 2.9. Measurements of actual leakage include the time span between October 2020 and February 2025. Observation of the construction site concludes a time series of the infiltration, however, because of inconsistency in data quality, an average is chosen. Therefore, infiltration is set to $1.5 \text{ (m}^3/\text{day)}$ with daily data points from January 1, 2017 to December 30, 2024.

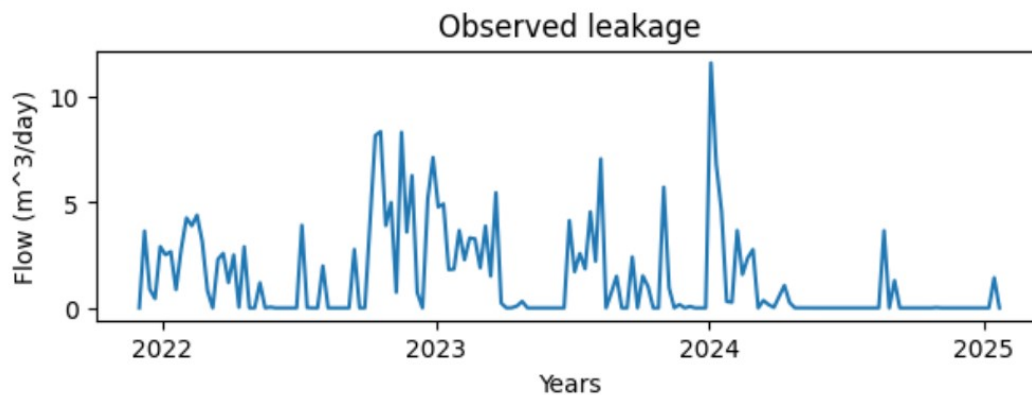


Figure 2.9: Graph of the observed leakage over time.

The leakage occurs primarily during the construction process and is measured at just over $10 \text{ (m}^3/\text{day)}$ at its highest point. It can be seen in Figure 2.9 that the flow decreases after 2024, which may indicate that measures have been taken to improve values. To seal the problem areas, concrete is injected with the purpose of filling the spaces, which counteracts and stops the flow of water (O. A. Chaudhari and G. Zirgulis, 2025).

2.5.3 Benchmark time series

Simulations in MODFLOW provide time series of both groundwater head as well as the flow of leakage and infiltration as described in Section 2.3.2. The benchmark

leakage time series is determined by the resulting flow value from the benchmark model and can be seen in Figure 2.10. Large disturbances originating from the Handels shaft had the greatest impact during a spike at the end of 2020 with up to $0.005 \text{ (m}^3/\text{s)}$. Leakage data from the benchmark model is higher than the observed values with a mean leakage of around $7 \text{ (m}^3/\text{s)}$ from the Handels shaft.

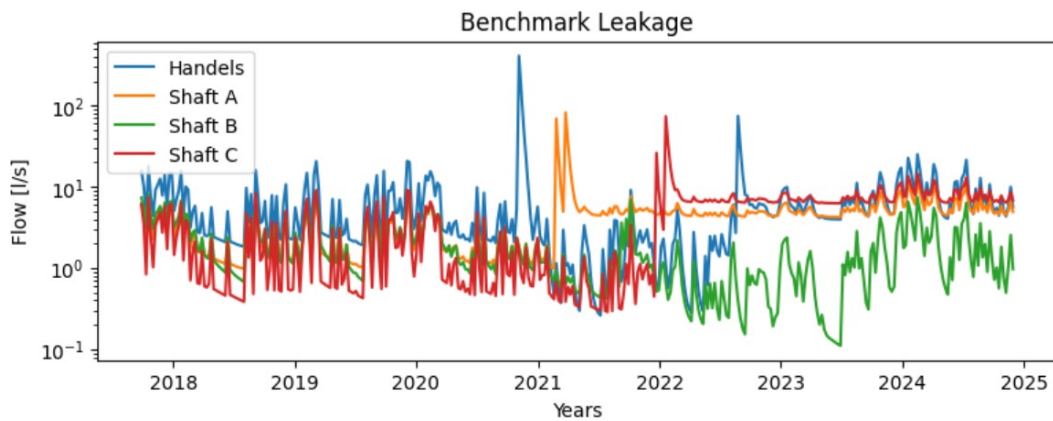


Figure 2.10: Graph of the groundwater leakage into modeled shafts from the benchmark model with logarithmic scale. Including the Handels shaft and shaft A, B and C.

2.5.4 Scenarios with synthetic shafts

To systematically evaluate the capability of the TFMs to detect specific disturbances to the groundwater head, multiple scenarios were introduced by including different combinations of the synthetic shafts, named A, B and C. The synthetic shafts are implemented in the benchmark model with similar hydraulic properties as the Handels shaft, but incorporated at different times and located at different locations to test the TFMs capabilities. This setup allows for controlled testing of the TFM’s ability to detect and distinguish multiple stress signals. Figure 2.7 shows an overview of where the synthetic shafts are located and Figure 2.8 shows a timeline of when each of the shafts are incorporated into the benchmark model, with a two-week temporal lag between each of the three modeled shaft segments.

The purpose of modeling time series with different combinations of synthetic shafts in different observation wells is to analyze how well the models can identify the disturbances from different distances. Table 2.2 presents all the tested scenarios for the different synthetic shafts. Identifying the influence of a specific shaft becomes increasingly challenging when multiple disturbances occur in a close time frame. Therefore, comparing scenarios with single and multiple shafts provides insight into the model’s accuracy and reliability. The performance of the TFMs in these scenarios is evaluated by analyzing residuals and model fit, as described in Section 3.3.2.

Scenario	Handels Shaft	Shaft A	Shaft B	Shaft C
Base	x			
A	x	x		
B	x		x	
C	x			x
AB	x	x	x	
AC	x	x		x
BC	x		x	x

Table 2.2: Table of all tested scenarios for the synthetic shafts A, B and C.

3

Results and Discussion

The following chapter presents the outcomes of the groundwater modeling made in the numerical model which serves as a benchmark model for a TFMs, as well as the results from the TFMs. Evaluations are presented and discussed of TFMs using both values from generated time series of constructed disturbances, fictional disturbances and also measured values to qualitatively assess the model.

3.1 Calibration of benchmark model

A benefit of using the DRN package to model the leakage into shafts is that the volume of water removed at each time step is recorded in MODFLOW's output files. This enables quantitative tracking of the drainage process throughout the simulation period. Additionally, drain volumes were visualized using ModelMuse by post-processing the cell-by-cell (CBC) output file. This allows the plotting of the drain rates in individual time steps across the model layers. The DRN package is also used to model storm water management within the modeled area. Previous calibrations inserted a large polygon above the model surface to stabilize the model and mimic storm water management, removing excess water that does not infiltrate the soil layers (Lilja and Zander, 2024). Figure 3.1 illustrates the drains during the one-week time step 259, starting 2022-09-08, in model row 71. The figure shows that the cell within the Handels shaft with the highest DRN flow has a flow of about $1.5 \times 10^{-5} \text{ m}^3/\text{s}$ while the Drains that represent the storm water management are about ten times lower. The entire Handels shaft has a total leakage flow of $1.65 \times 10^{-4} \text{ m}^3/\text{s}$ during the same time step, 259.

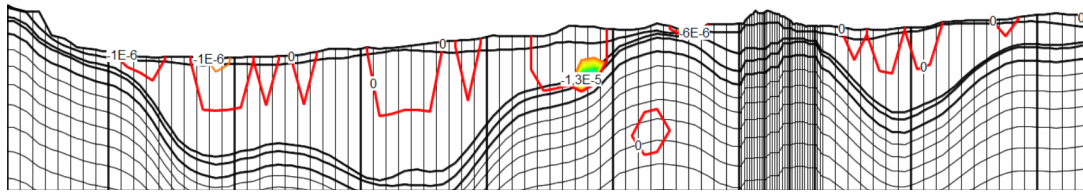


Figure 3.1: Groundwater flow out from the MODFLOW model caused by DRN package during one week, starting 2022-09-08, in model row 71 in m^3/s . Plotted in ModelMuse through the model layers and cells, represented in black.

Through iterative calibrations, the model was adjusted to match the observed leakage rates into the shaft. A satisfactory match was achieved when the shaft bottom was assigned a hydraulic conductivity of 1×10^{-8} m/s, and the shaft walls, represented by the HFB package with a thickness of one meter, were assigned a conductivity of 1×10^{-10} m/s. These values fall within the range reported for similar engineered structures in other hydrogeological modeling studies (Dada and Uchechukwu, 2016, Luca et al., 2024). The resulting model configuration produced an average simulated groundwater leakage into the Handels shaft of approximately 3.8 l/min. Figure 2.10 shows the numerical simulated leakage into both the Handels shaft and the synthetic shafts that are modeled with the Handels shaft as a reference.

The most effective of the three infiltration wells at the site, HH7449U, was configured to infiltrate when the groundwater level ranged between +12.5 and +12.8 m (Hagman et al., 2024). By the end of October 2023, the mean infiltration rate from this well was approximately 5.1 l/min. However, when implemented in the benchmark model with a fixed groundwater level of 13 m, the resulting infiltration was significantly lower, about 0.005 l/min due to the already elevated groundwater head in the area. As a result, only the most effective infiltration well, HH7449U, was included in the model.

3.2 Observational time series

Figure 3.2 shows a TFM calibrated on measured values for the well HH4117U, located south east of the Handels shaft (see Figure 3.3). An extract of a borehole has been made to only the borehole HH4117U with the extended list of borehole in Appendix C.1. The correlation coefficient R^2 for the HH4117U model was calculated to 65.78 %, indicating a moderate agreement between the measured and simulated groundwater levels. The residuals plots show localized deviations between modeled and observed head, especially during sharp peaks in the measured values. These deviations may reflect disturbances that are present in reality but not fully captured by the MODFLOW benchmark model. For instance, temporary construction activities or changes in drainage infrastructure could cause fluctuations not included

in the benchmark simulation.

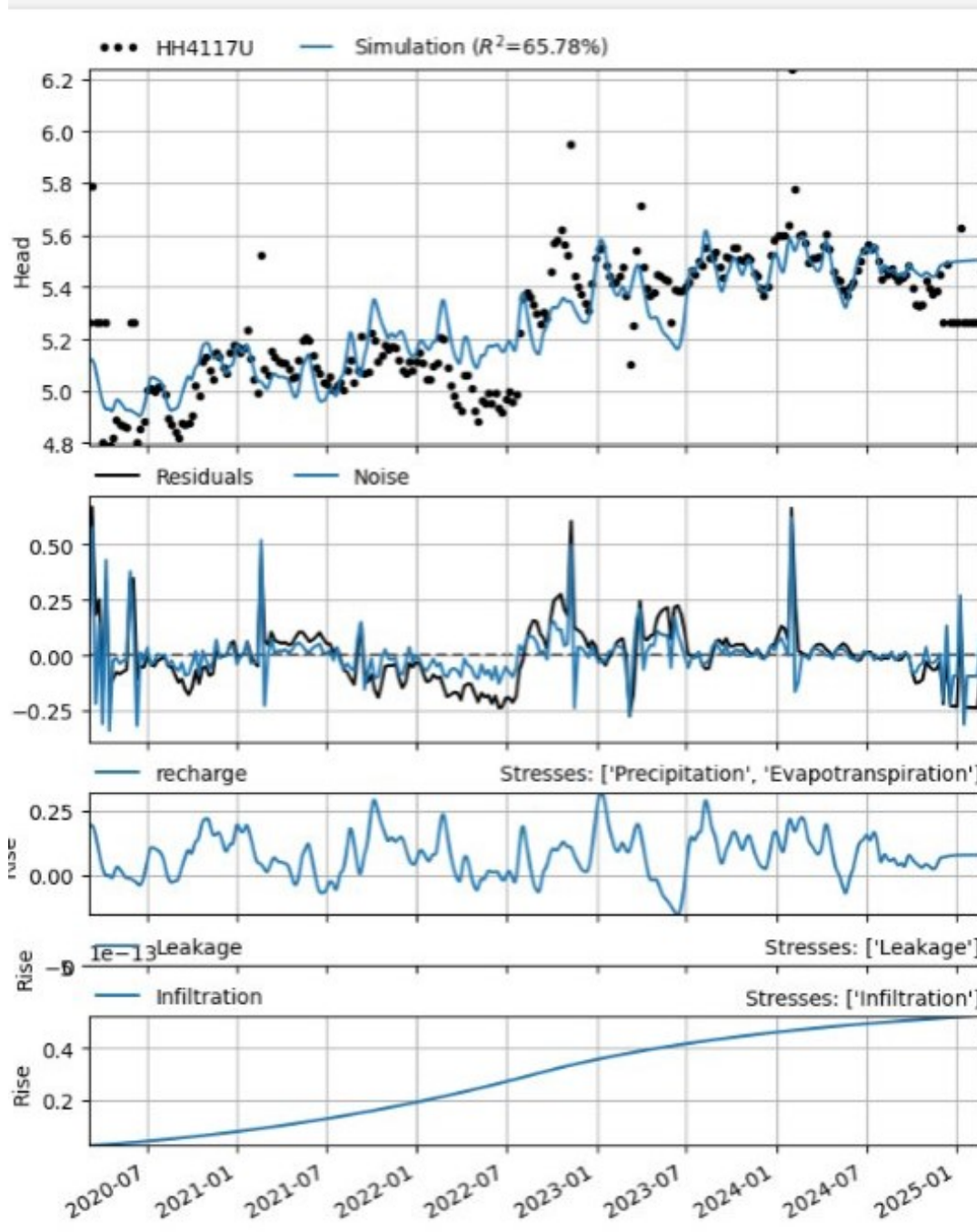


Figure 3.2: TFM simulation based on measured values for borehole HH4117U.

The TFM based on measured data are missing several significant real-world disturbances, which is evident across all simulations. This highlights a key limitation of modeling based on a benchmark model when the purpose of the model is to detect and distinguish specific disturbances. Recharge produces significant responses

in the TFM simulations based on measured values, sometimes resulting in larger modeled effects on groundwater levels than what is observed in the measured data. This suggests that the TFM may overestimate the influence of recharge when other disturbances are not fully captured or included as stresses. Although still having significant limitations, the model simulates the groundwater head with appropriate magnitude, indicating that the TFM can be used for some limited case scenarios at a study site.

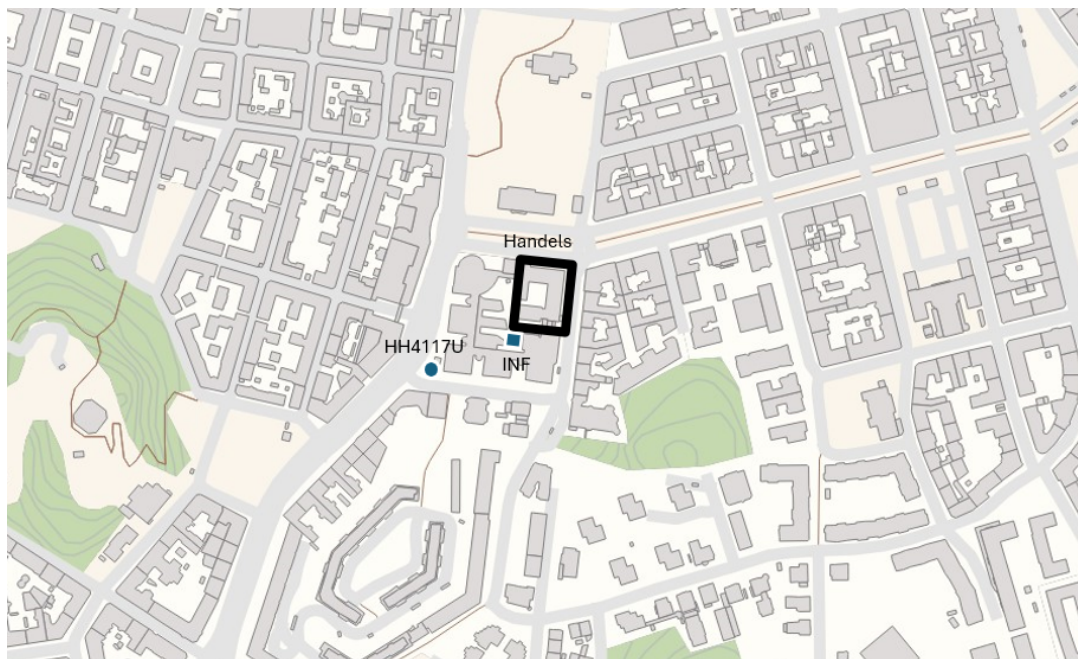


Figure 3.3: Situation map of the TFM simulated borehole HH4117U together with the Handels shaft and infiltration well.

3.3 Scenarios with synthetic shafts

This section presents the modeling results of the TFM, based on time series generated by the benchmark model. Scenarios involving different combinations of synthetic disturbances (as shown in Table 2.2), are simulated and compared.

3.3.1 Plotted transfer function models with all synthetic shafts

Figure 3.4 shows the results of the TFM simulation for borehole HH4117U, where all synthetic shaft disturbances (A, B, and C), as well as the Handels shaft, recharge, and infiltration, are included as stress inputs. The model achieves a high correlation coefficient of $R^2 = 87.00\%$. The models including the synthetic shafts in different combinations have in general a similar correlation coefficient, compared to the

models only including the constructed disturbances. Additional models include the synthetic shafts are presented in Appendix C.3.

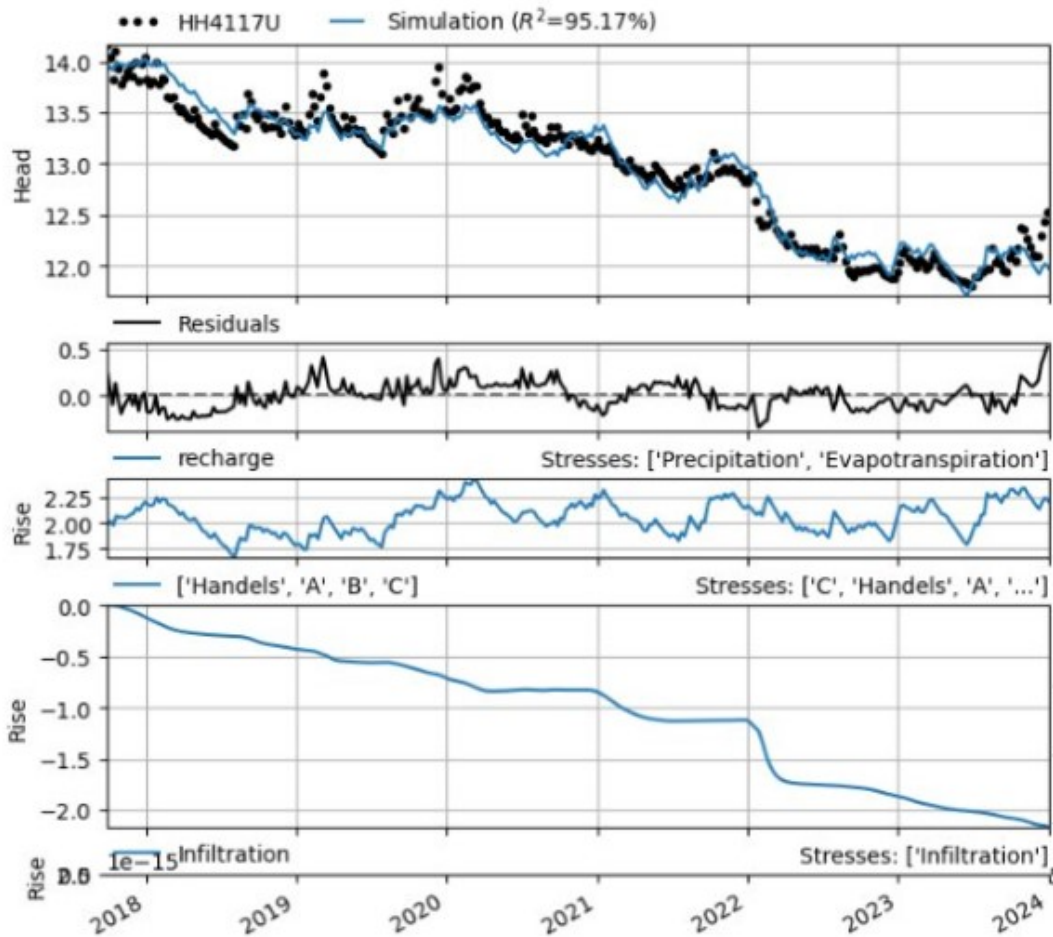


Figure 3.4: TFM simulation based on benchmark generated values for HH4117U with fictional disturbances of A,B & C shafts.

3.3.2 Identification of impact of synthetic shafts

The first graph in Figure 3.5 show the residual for all six scenarios. For example, scenario A consists of a TFM simulation in which the Handels shaft and shaft A constitute leakage stress.

To be able to detect outliers or deviations, the values are compared to the base scenario, with only the Handels shaft included. The difference in residuals conducts abnormal effects on the groundwater head. A positive value in residual means that the groundwater head from input data is higher than the simulation with TFM related to variation in leakage stresses. Figure 3.6, 3.8 and 3.11 therefore describe the deviation in groundwater head from the base scenario, generated in the benchmark model, to the TFM simulation with the variance of leakage based on scenarios.

3. Results and Discussion

Figure 3.5 and 3.6 shows results from the previously established HH4117U, located close to shaft B and furthest to shaft A. Declines in the groundwater head occurs in the year 2021 with further reduction when adding shaft C (see Figure 3.5). The greatest disturbances occur in scenario C, with groundwater levels depress 0.3 m lower than when only the Handels shaft is constructed. The change can be seen as insignificant compare to the total loss of 2 m when all disturbances are active, shown in section 3.3.

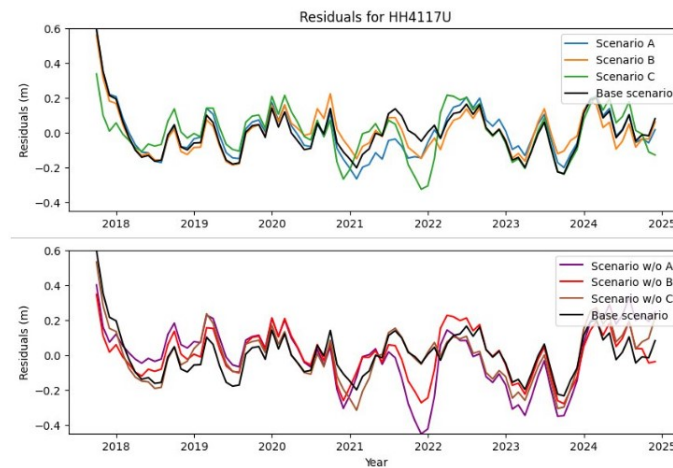


Figure 3.5: Residuals from TFM simulations with different scenarios for HH4117U.

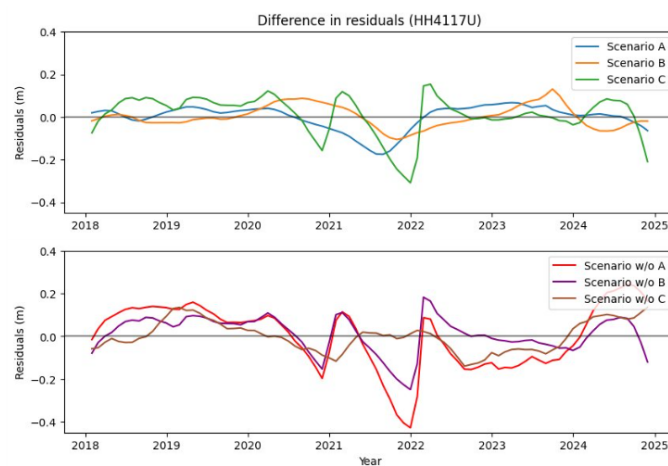


Figure 3.6: Difference in residuals from the scenarios compared to the base scenario for HH4117U. Values are taken from the benchmark model.

The well HH4266U is located north of the Handels shaft, partially further away from shaft B in the south. Results of simulations of the different scenarios for well HH4266U are presented in Figures 3.7 and 3.8. The similar result in residuals between base scenario and scenario A and B proves that the synthetic shafts A and B are not causing additional disturbances in the groundwater table for this well. Scenario C accounts for more significant disturbances compared to the other scenarios, as shown in Figure 3.8.

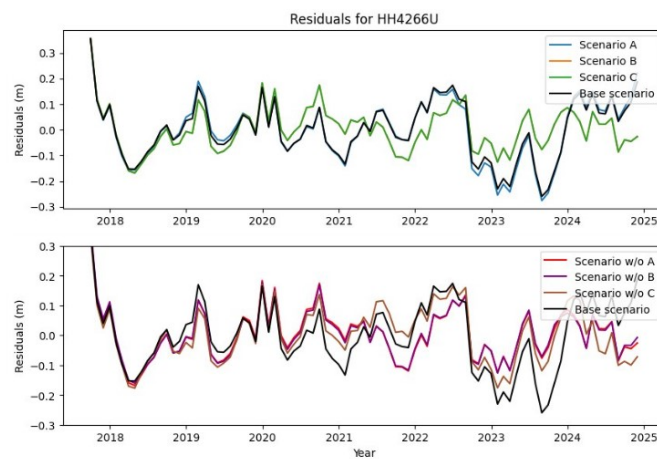


Figure 3.7: Residuals from TFM simulations with different scenarios for HH4266U.

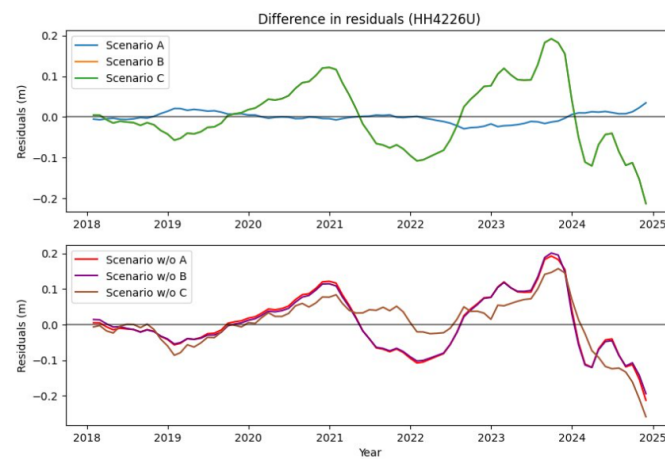


Figure 3.8: Difference in residuals from the scenarios compared to the base scenario for HH4266U. Values are taken from the benchmark model.

Figures 3.10 and 3.11 show results from HH7453U, located east of the Handels shaft (see Figure 3.9). The well has the same distance to shaft A, B and C. Scenario B for the well has a trendline with a residual close to 0 shown in Figure 3.10. Similar results are found in the scenario without shaft A and the scenario without shaft C. In Figure 3.11, Scenario B deviates significantly, with values reaching up to 0.8 m above the base scenario. However, due to the large distance between the borehole and the stress source, shaft B, this deviation may not necessarily indicate a true disturbance. Figure 3.11 show that scenarios A and C are close to the base scenario. The impact that shaft A and C have on this well's groundwater head is insignificant.

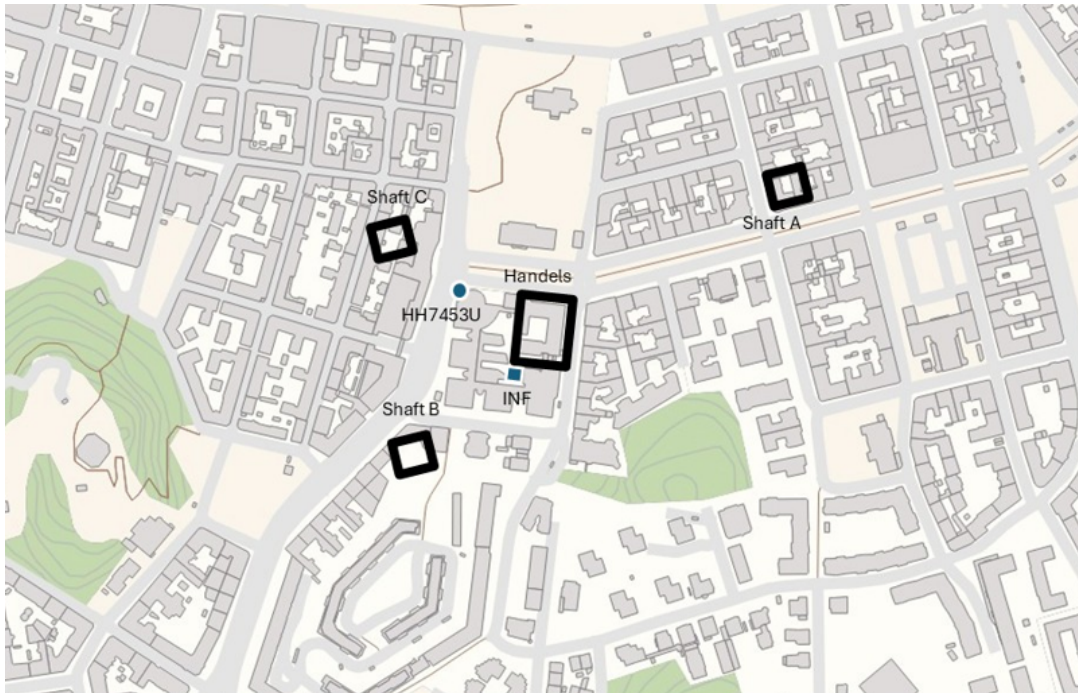


Figure 3.9: Situation map of the TFM simulated borehole HH7453U together with the Handels shaft, infiltration well and synthetic shafts.

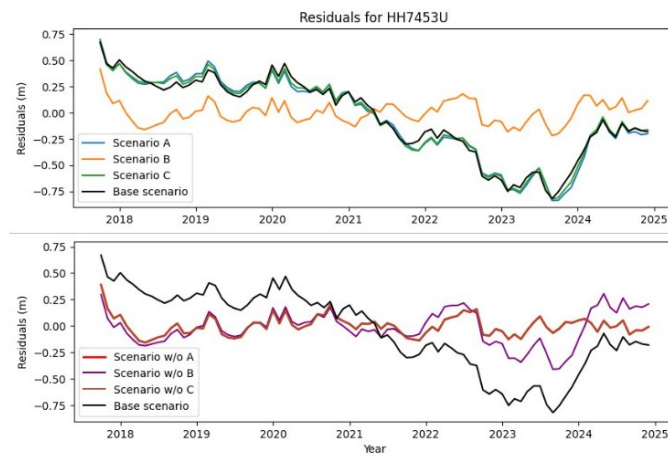


Figure 3.10: Residuals from TFM simulation with different scenarios for HH7453U.

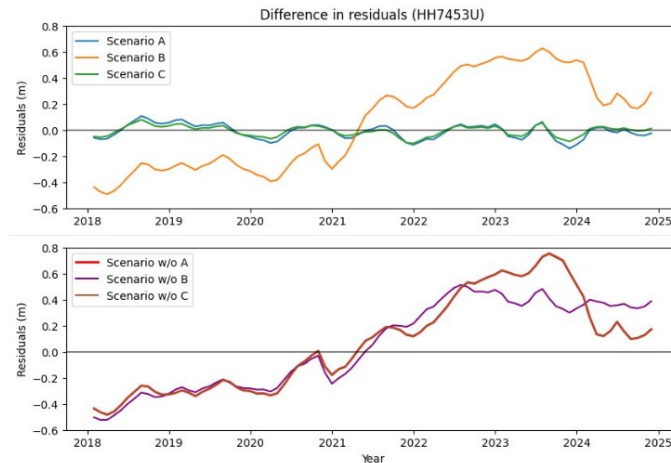


Figure 3.11: Difference in residuals from the scenarios compared to the base scenario for HH7453U. Values are taken from the benchmark model.

Shaft C has proven to affect the groundwater table the most for the first and second presented wells, HH4117U and HH4266U. This suggests that the added stress of shaft C, causes a drawdown in the groundwater table when constructed. However, inconsistencies do present themselves for the last well, HH7453H, which is the one closest to shaft C but did not show a clear drawdown.

3.4 Implications for transfer function analysis of perturbed time series

The most significant advantages in developing transfer function models compared to numerical models is their simplicity and low amounts of inputs needed. Transfer function models could be implemented in the early stages of a project at an urban site for preliminary impact assessments, without a large amount of field measurements. However, the results indicate that the transfer function models developed in TFM have limitations in assessing hydrogeological disturbances with high precision.

The TFMs based on time series from the benchmark model generally overestimated the effect of recharge post calibration, as can be seen in Figure 3.12 and 3.13. Additional simulations can be seen in Appendix C.2.1. This could be due to the difference in how the recharge is implemented in the TFM versus the benchmark model. The numerical benchmark model uses the MODFLOW RCH package which takes both runoff and evaporation into account; only the water that infiltrates through the unsaturated zone recharges the groundwater (Winston, 2023). This is in contrast to TFMs where all water that have been calculated as recharge stress, explained in section 2.5, produces groundwater (Collenteur et al., 2019). As described in section 2.3.1, stormwater management is specifically modeled with the DRN package in the benchmark model, which could be the reason for the overestimation of recharge post calibration of the TFMs.

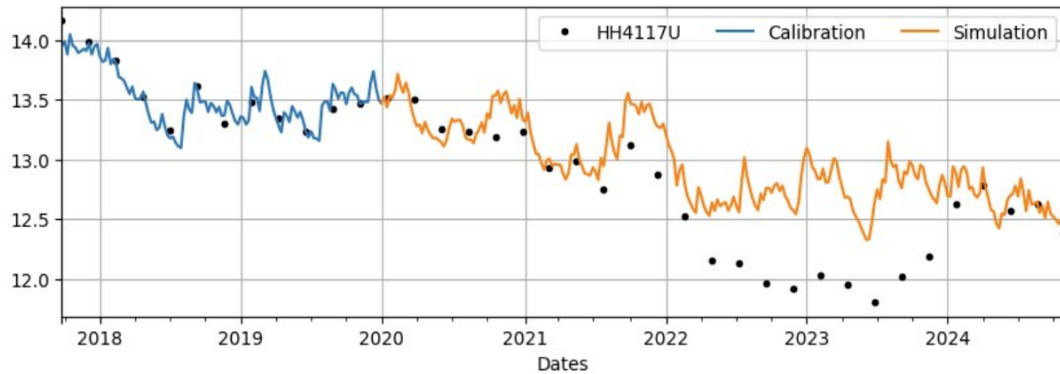


Figure 3.12: TFM simulation with limited calibration based on simulated values for HH4117U.

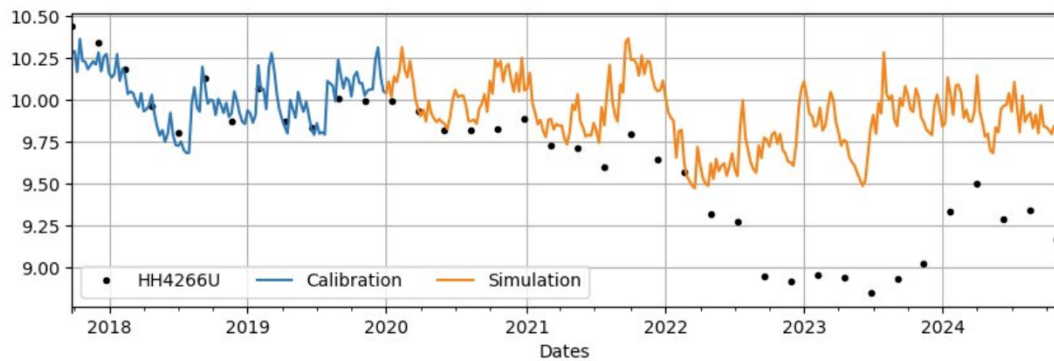


Figure 3.13: TFM simulation with limited calibration based on simulated values for HH4266U.

Furthermore, the study relies on an existing numerical model. As such, its accuracy is constrained by the assumptions, simplifications, and structural limitations inherent in that model. The reliability of the results also depends on the quality of field measurements used for model calibration and validation, which may introduce uncertainty. The scope of the study is also geographically limited to the Haga Station site within the Västlänken infrastructure project and its immediate surroundings. Findings may therefore not be directly generalizable to other geological or hydrological contexts. Due to these constraints, a transfer function model could be implemented in conjunction with a numerical model for preliminary impact assessment of disturbances to the groundwater table.

3.5 Outlook

The synthetic shaft scenarios were designed to isolate and evaluate the TFM under simulated conditions. Although effective for benchmarking, they may not fully capture the complexity of real hydrogeological environments. Expanding this approach to include more diverse geological settings, variable shaft geometries, and different types of disturbances would help generalize the applicability of transfer function modeling across a wider range of infrastructure projects. Future work should also focus on integrating additional stresses and exploring automated methods for disturbance detection based on variance recognition in residual time series. Finally, further sensitivity analyses could be conducted to evaluate the impact of calibration periods on the transfer function model performance. These insights would help refine the methodology for implementing data-driven groundwater models in infrastructure projects.

4

Conclusion

This study evaluated the ability of a data-driven transfer function model, implemented through the Pastas framework, to model groundwater head time series and detect disturbances related to excavation. Transfer function models were developed using both observed and synthetically generated data to assess their performances in identifying the effects on groundwater of implemented excavation shafts. Haga Station, part of the Västlänken project, served as the study site where a previously validated numerical model developed in MODFLOW was extended. This numerical model acted as a benchmark for generating time series of groundwater head, shaft leakage, and infiltration flow. The transfer function models were calibrated and applied to a variety of scenarios involving both real and synthetic disturbances. These simulations were used to compare model performance, particularly through analysis of residuals to evaluate the model's capability to detect and distinguish different sources of groundwater disturbances.

The simulations demonstrated that the transfer function models are capable of replicating groundwater head behavior by using initial groundwater levels in combination with recharge, shaft leakage, and infiltration flow as stress inputs. TFMs based on observed values from site studies concluded the rationale for using the numerical model as benchmark for assessing the capabilities of transfer function models at the study site. However, certain limitations were noted, including the absence of some temporary real-world disturbances and a tendency to overestimate the influence of recharge. When the TFMs for boreholes were calibrated on undisturbed time series and subsequently applied to simulate groundwater head during the influence of constructed disturbances, they consistently underestimated the effect of leakage. This indicates that the transfer function model may have difficulty accurately capturing the magnitude of the drawdown when disturbance stresses are introduced.

Introducing synthetic disturbances provided theoretical scenarios with comparisons of the groundwater time series from base scenarios, outliers could be identified. The transfer function model was useful to some extent in visualizing groundwater fluctuations and identifying the sources of those disturbances. However, a large inconsistency presented itself with iteration with additional wells. Low correlation of how added disturbances could affect groundwater head in a close observation well indicates imprecision in TFM as a modeling tool for this study.

Overall, this type of transfer function modeling tool has the potential to be valuable for predicting groundwater drawdown when affected by anthropogenic stresses,

4. Conclusion

especially when considering the lower number of variables needed to calibrate it. Although, significant irregularities in the model's reliability raise concerns regarding its application in real-world scenarios.

Bibliography

- Allen, R. G., Pereira, L. S., Raes, D., & Smith, M. (1998). *Crop evapotranspiration: Guidelines for computing crop water requirements* (Vol. 56) [FAO, Rome, 300(9), D05109]. FAO.
- Anderson, M. P., Woessner, W. W., & Hunt, R. J. (2015). *Applied groundwater modeling - simulation of flow and advective transport (2nd edition)*. Elsevier. <https://app.knovel.com/hotlink/toc/id:kpAGMSFAT1/applied-groundwater-modeling/applied-groundwater-modeling>
- Bakker, M., & Schaars, F. (2019). *Solving groundwater flow problems with time series analysis: You may not even need another model*. National Groundwater Association.
- Collenteur, R. A., Bakker, M., Caljé, R., Klop, S. A., & Schaars, F. (2019). Pastas: Open source software for the analysis of groundwater time series. *Groundwater*, 57(6), 877–885. <https://doi.org/10.1111/gwat.12925>
- Collenteur, R. A., Bakker, M., Klammler, G., & Birk, S. (2021). Estimation of groundwater recharge from groundwater levels using nonlinear transfer function noise models and comparison to lysimeter data. *Hydrology and Earth System Sciences*, 25, 2931–2949. <https://doi.org/10.5194/hess-25-2931-2021>
- Collenteur, R. A., Haaf, E., Bakker, M., Liesch, T., Wunsch, A., Soonthornrangsang, J., White, J., Martin, N., Hugman, R., de Sousa, E., Vanden Berghe, D., Fan, X., Peterson, T. J., Bikše, J., Di Ciacca, A., Wang, X., Zheng, Y., Nölscher, M., Koch, J., ... Meysami, R. (2024). Data-driven modelling of hydraulic-head time series: Results and lessons learned from the 2022 groundwater time series modelling challenge. *Hydrology and Earth System Sciences*, 28(23), 5193–5208. <https://doi.org/10.5194/hess-28-5193-2024>
- Condon, L. E., Kollet, S., Bierkens, M. F. P., Fogg, G. E., Maxwell, R. M., Hill, M. C., et al. (2021). Global groundwater modeling and monitoring: Opportunities and challenges. *Water Resources Research*, 57, e2020WR029500. <https://doi.org/10.1029/2020WR029500>
- Dada, O., & Uchekukwu, E. (2016). Hydraulic conductivity of compacted laterite treated with iron ore tailings [Open Access under CC BY 4.0 license]. *Advances in Civil Engineering*, 2016, 1–8. <https://doi.org/10.1155/2016/4275736>
- Haaf, E., Ericsson, L., Sundell, J., Liljedahl, L. C., & Selroos, J.-O. (2025). Some insights from modeling groundwater levels in open boreholes in crystalline rock in tunneling projects [Open Access under CC BY-NC-ND 4.0 license]. In J. et al. (Ed.), *Tunnelling into a sustainable future – methods and technologies*

- (pp. 3732–3739). Taylor & Francis. <https://doi.org/10.1201/9781003559047-475>
- Haaf, E., Giese, M., Reimann, T., & Barthel, R. (2023). Data-driven estimation of groundwater level time-series at unmonitored sites using comparative regional analysis. *Water Resources Research*, 59(e2022WR033470). <https://doi.org/10.1029/2022WR033470>
- Hagman, H., Larsson, J., & Ekberg, J. (2024, December). *Pm grundvattennivåer månadsavstämning november 2024, handelsschaktet* [Unpublished report, Tyréns AB, for Trafikverket project Västlänken och Olskroken planskildhet] [Internal project document BBP05-50GT-025-0500-0_0-0059], Tyréns AB.
- Harbaugh, A. W. (2005). *Modflow-2005, the us geological survey modular groundwater model: The ground-water flow process* (tech. rep.). US Department of the Interior. US Geological Survey Reston, VA, USA.
- Lilja, E., & Zander, Z. (2024). *Towards benchmarking time series analysis with process-based groundwater models: The case of hydrogeological impacts of tunnel construction* [Master's Thesis]. Department of Architecture, Civil Engineering, Division of Geology, and Geotechnics. <https://www.chalmers.se>
- Lindblom, A., & Boström, L. (2021). *Evaluating transfer-function models to understand groundwater level impacts* [MSc thesis in Infrastructure and Environmental Engineering]. Chalmers University of Technology. <https://hdl.handle.net/20.500.12380/302874>
- Luca, C. D., Pignalosa, A., & Budetta, P. (2024). Evaluating rock mass groutability at shallow depths: A novel approach based on geo-structural surveys and permeability tests [Open Access under CC BY 4.0 license]. *Bulletin of Engineering Geology and the Environment*, 83(4), 83–123. <https://doi.org/10.1007/s10064-024-03600-5>
- Niswonger, R. G., Panday, S., & Ibaraki, M. (2011). *Modflow-nwt, a newton formulation for modflow-2005* (tech. rep. No. Techniques and Methods 6-A37) (U.S. Geological Survey Techniques and Methods 6-A37). U.S. Geological Survey. Reston, Virginia. <https://pubs.usgs.gov/tm/tm6a37/>
- O. A. Chaudhari and G. Zirgulis. (2025). Cementbaserad injektering (material, injekteringsmetoder och mätningar). <https://www.ri.se/sv/expertisomraden/expertiser/cementbaserad-injektering>
- Omoko, E., Okeke, O., & Opara, K. (2018). *A review of the mechanism and engineering/environmental problems of subsidence due to groundwater extraction* (tech. rep.). Department of Geology, Federal University of Technology. Owerri.
- Onyutha, C. (2022). A hydrological model skill score and revised r-squared. *Hydrology Research*, 53(1), 51–62. <https://doi.org/10.2166/nh.2021.071>
- Panda, G. P., & Vipulanandan, C. (2019). *Factors influencing surface soil settlement due to dewatering* (tech. rep.). University of Houston, Department of Civil and Environmental Engineering. Houston, Texas.
- Reilly, T. E., & Harbaugh, A. W. (2004). *Guidelines for evaluating ground-water flow models* (tech. rep. No. 2004–5038). U.S. Geological Survey. Reston, Virginia. <https://doi.org/10.3133/sir20045038>

- Schoenfeld, A. H. (1998). Making mathematics and making pasta: From cookbook procedures to really cooking. In J. G. Greeno & S. V. Goldman (Eds.), *Thinking practices in mathematics and science learning* (1st, p. 21). Routledge.
- SMHI. (2025). Ladda ner meteorologiska observationer [Accessed: 2025-03-21]. <https://www.smhi.se/data/hitta-data-for-en-plats/ladda-ner-vaderobservationer/precipitation24HourSum/71420>
- Sun, J., Hu, L., Li, D., Sun, K., & Yang, Z. (2022). Data-driven models for accurate groundwater level prediction and their practical significance in groundwater management. *Journal of Hydrology*, 608, 127630. <https://doi.org/10.1016/j.jhydrol.2022.127630>
- Sundkvist, U., & Wallroth, T. (2016). *Pm hydrogeologi: Ansökan om tillstånd enligt miljöbalken för anläggandet av västlänken och olskroken planskildhet, göteborgs stad, mölndals stad, västra götaland län* (Technical Report No. TRV 2016/3151) (Retrieved from https://bransch.trafikverket.se/contentassets/623cad16101d40edbc580de82cd93ee6/pm_hydrogeologi.pdf). Trafikverket.
- Trafikverket. (2020). Västlänken: Informationsmaterial – deletapp haga [Accessed: 2025-05-15]. https://bransch.trafikverket.se/contentassets/034b94284d984fa48aea6f12ae610f8kompodium_deletapp_haga_a4_tryck.pdf
- Trafikverket. (2021). Västlänken: The stations and the tunnel [Accessed: 2025-04-17]. <https://bransch.trafikverket.se/en/startpage/projects/Railway-construction-projects/The-West-Link-ProjectVastlanken/The-stations-and-the-tunnel/>
- USGS. (2022). Modflow and related programs [Retrieved from USGS 4/4/2025]. <https://www.usgs.gov/mission-areas/water-resources/science/modflow-and-related-programs>
- Vonk, M. A., Collenteur, R. A., Panday, S., Schaars, F., & Bakker, M. (2024). Time series analysis of nonlinear head dynamics using synthetic data generated with a variably saturated model. *Groundwater*, 62(5), 748–760. <https://doi.org/10.1111/gwat.13403>
- Wikby, P., Haaf, E., Abed, A., Rosén, L., Sundell, J., & Karstunen, M. (2024). A grid-based methodology for the assessment of time-dependent building damage at large scale. *Tunnelling and Underground Space Technology*, 149, 105788. <https://doi.org/10.1016/j.tust.2024.105788>
- Winston, R. B. (2023). *Getting started with modflow*. The Groundwater Project. <https://doi.org/10.21083/978-1-77470-030-3>

A

Plotted graphs

A.1 Evapotranspiration

Evapotranspiration, calculated by using Eto-package in Python can be seen plotted in figure bellow.

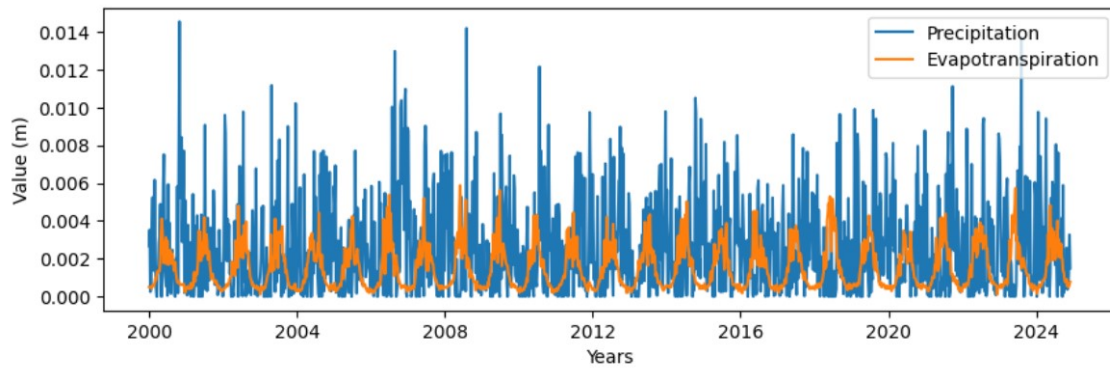


Figure A.1: The amount of PET (m/day) over time.

B

Appendix: Python code

Python code used for calculation Evapotranspiration and to conduct the datadriven Pastas model can be seen in appendix A. Code for plotting results and is also shown for transparency.

B.1 Eto

The code for calculating PET is shown in the following Appendix. Input data includes solar radiation, Rs, Relative humidity, Rh and temperature within the time-frame 2000-01-01 to 2024-12-31.

Conversion of the units and prefix is done to meet the correct required units of the input data.

```
1 # Import packages
2
3 from eto import ETo, datasets
4 import openpyxl
5 import numpy as np
6 import matplotlib.pyplot as plt
7 et1 = ETo()
8 import math
9
10 # Import climate data
11
12 # Relative humidity [-]
13 R_h = pd.read_excel(r'C:\Line-of-path-to-file\relative_humidity.xlsx',
14                    parse_dates=[0], index_col=0)
15
16 # Solar radiation, Rs [J/m^2]
17 R_s = pd.read_excel(r'C:\Line-of-path-to-file\solar_radiation.xlsx',
18                    parse_dates=[0], index_col=0)
19
20 R_h = R_h.groupby("Dates") # Group by day
21 R_h = R_h["R_h"].mean().reset_index()
22
23 R_s = R_s.groupby("Dates") # Group by day
24 R_s = R_s["R_s"].mean().reset_index()
25
26
27 R_s['R_s'] *= 1e-6 # Multiply 'R_s' by 10^-6 to get unit [MJ/m^2]
28
```

B. Appendix: Python code

```
29
30 # Temperature, min and max, [celcius]
31 Temp = pd.read_excel(r'C:\Line-of-path-to-file\temperature.xlsx',
    parse_dates=[0], index_col=0)
```

Eto is then used calculate the vapotrasporation with the given climate data. Evap-otransporation is concluded with datapoints for each day.

```
1 # Merge all dataframes on 'Dates' column
2 Eto= R_h.merge(R_s, on="Dates", how="outer") \
3     .merge(Temp, on="Dates", how="outer")
4
5 # Handle missing values (e.g., fill with mean or drop)
6 Eto =Eto.ffill().bfill()
7
8 Eto['e_s_min'] = 0.6108*np.exp((17.27*Eto['T_min'])/(Eto['T_min']
9     ]+237.3))
10 Eto['e_s_max'] = 0.6108*np.exp((17.27*Eto['T_max'])/(Eto['T_max']
11     ]+237.3))
12
13 Eto['e_s'] = ((Eto['e_s_min'] + Eto['e_s_max']) / 2)
14
15 Eto['e_a'] = ((Eto['e_s']* Eto['R_h']) / 100)
16
17
18 R_h = Eto["R_h"]
19 R_s = Eto["R_s"]
20 T_min = Eto["T_min"]
21 T_max = Eto["T_max"]
22 e_a = Eto["e_a"]
23
24 Eto.tail(30) #viewing dataframe
```

Geographical data is taken from SMHI (2025), descriptions of measuring station. The dataframes included datapoints for each day in current calculations. For R_s , would this mean the total amount of solar radiance during the whole day in MJ/m². The frequency is theirfor defind as daily in the code.

```
1 # Geographical data
2 freq='D'           #frequency where ''D stands for day
3 z_msl=3.038        #height above sealevel (weather station Goteborg A)
4 lat=57.7156        #latitude (weather station Goteborg A)
5 lon= 11.9924       #longitude (weather station Gteborg A)
6 TZ_lon=15          #time zone (weather station Gteborg A)
```

Calculations for evapotransporations require a dataframe with selected parameters. The parameters used are relative solar, R_s (Mj/m²) the maximum and minimum temperature (celsius) and vapour pressure, e_a (-).

```
1 # Eto calculations
2 Eto_indata = pd.concat([R_s, T_max, T_min, e_a], axis=1) # fitting
3     data
4
5 # Create a new DateTime index starting from '2000-01-01'
6 Eto_indata.index = pd.date_range(start='2000-01-01', periods=len(
7     Eto_indata), freq='D')
```

```

6
7 # Set the name of the index
8 Eto_indata.index.name = "Dates"
9 Eto_indata

```

To obtain correct input data for the calculations and counteract missing values is a test-code conducted. If values is missing from a parameter's dataset, it can be filled with mean values after investigation of faulty during extraction of values.

```

1 # Check for missing values in each data frame
2 print(R_h.isnull().sum())
3 print(R_s.isnull().sum())
4 print(Temp.isnull().sum())
5 print(e_a.isnull().sum())

1 # Create an instance of the ParamEst class
2 #et1 = ETo.ParamEst()
3
4 # Parameter estimation function
5 et1.param_est(Eto_indata, freq, z_msl, lat,lon,TZ_lon=None)
6 # view the first five rows of the estimated parameters
7 etlist=et1.ts_param.head()

```

```

1 # Calculation and plotting
2
3 evp=et1.eto_fao()
4
5 # plotting the results
6 evp.plot(label='ETo', figsize=(10,4))
7 plt.legend(ncol=1,loc=0)
8
9 # Save the dataframe as 'evap' in the specified location
10
11 evp.name = 'Evap'
12
13
14 evp.to_excel(r'C:Line-of-path-to-file\evap.xlsx')

```

B.2 Appendix: Recharge and plotting

Recharge is calculated in Python and with the forming cod. The results of the calculation are used as stress in Pastas models.

```

1 #Evapotranspiration [m/day]
2 Evap = pd.read_excel(r'C:Line-of-path-to-file\evap.xlsx', parse_dates
   = [0], index_col=0) # from Eto calculations
3 Evap = Evap.resample('7D').mean() # changing ot weekly data
4
5 # Precipitation [m/day]
6 Prec = pd.read_excel(r'C:Line-of-path-to-file\prec.xlsx', parse_dates
   = [0], index_col=0)
7 Prec = Prec.resample('7D').mean() # changing ot weekly data
8
9 # Combine Evap and Prec into one dataframe
10 Climatedata = pd.concat([Evap, Prec], axis=1)

```

```
11
12 # Rename columns
13 Climatedata.columns = ['Evapotranspiration', 'Precipitation']
14
15 # Calculate Recharge
16 Climatedata['Recharge'] = Climatedata['Precipitation'] - Climatedata['
    Evapotranspiration']
17
18 # Defining dataframe
19 Rech = Climatedata['Recharge']
20
21 # Plot Recharge
22 plt.figure(figsize=(12, 4))
23 Rech.plot(color='green')
24 plt.xlabel("Time [years]")
25 plt.ylabel("Recharge (m/day)");
26 plt.legend(['Recharge'])
```

B.3 Appendix: Python code for measured values

The Pastas models for the measured values. The time series of the groundwater head is based on the observed value which has occurred in real life. The following code is behind the plots shown in 3.2. Further Pastas usage can be found in *Making mathematics and making pasta: From cookbook procedures to really cooking* by Schoenfeld (1998).

```
1
2 # Importing packages
3 import pandas as pd
4 import pastas as ps
5 import numpy as np
6 import matplotlib.pyplot as plt
7 import math
8 from scipy import stats
9 from scipy.spatial.distance import cdist
10 import matplotlib.pyplot as plt
11
12
13 # Read data from excel files
14 HH4117U = pd.read_excel(r'C:\Line-of-path-to-file\HH4117U.xlsx',
    parse_dates=[0], index_col=0)
15 HH4266U = pd.read_excel(r'C:\Line-of-path-to-file\HH4266U.xlsx',
    parse_dates=[0], index_col=0)
16 HH7453U = pd.read_excel(r'C:\Line-of-path-to-file\HH7453U.xlsx',
    parse_dates=[0], index_col=0)
17 HH7455U = pd.read_excel(r'C:\Line-of-path-to-file\HH7455U.xlsx',
    parse_dates=[0], index_col=0)
18
19
20 # Group the datapoints to remove multiple datapoints on one day
21 # Change them to weekly data points
22 # Remove all datapoints before the date 2020-03-01
23
24 # HH4117U
```

```

25 HH4117U = HH4117U.groupby("Dates")
26 HH4117U = HH4117U["HH4117U"].mean().reset_index()
27 HH4117U.set_index("Dates", inplace=True)
28 HH4117U = HH4117U.resample('7D').mean()
29 HH4117U = HH4117U.loc['2020-03-01':]
30
31 # HH4266U
32 HH4266U = HH4266U.groupby("Dates")
33 HH4266U = HH4266U["HH4266U"].mean().reset_index()
34 HH4266U.set_index("Dates", inplace=True)
35 HH4266U = HH4266U.resample('7D').mean()
36 HH4266U = HH4266U.loc['2020-03-01':]
37
38 # HH7453U
39 HH7453U = HH7453U.groupby("Dates")
40 HH7453U = HH7453U["HH7453U"].mean().reset_index()
41 HH7453U.set_index("Dates", inplace=True)
42 HH7453U = HH7453U.resample('7D').mean()
43 HH7453U = HH7453U.loc['2020-03-01':]
44
45 # HH7455U
46 HH7455U = HH7455U.groupby("Dates")
47 HH7455U = HH7455U["HH7455U"].mean().reset_index()
48 HH7455U.set_index("Dates", inplace=True)
49 HH7455U = HH7455U.resample('7D').mean()
50 HH7455U = HH7455U.loc['2020-03-01':]
51
52
53 # Fill NaN values with mean value for HH4117U
54 HH4117U = HH4117U.fillna(HH4117U.mean())
55
56 # Fill NaN values with mean value for HH4266U
57 HH4266U = HH4266U.fillna(HH4266U.mean())
58
59 # Fill NaN values with mean value for HH7453U
60 HH7453U = HH7453U.fillna(HH7453U.mean())
61
62 # Fill NaN values with mean value for HH7455U
63 HH7455U = HH7455U.fillna(HH7455U.mean())
64
65
66 # Check for NaN values in the dataframes
67
68 nan_values_HH4117U = HH4117U.isnull().sum().sum()
69 nan_values_HH4266U = HH4266U.isnull().sum().sum()
70 nan_values_HH7453U = HH7453U.isnull().sum().sum()
71 nan_values_HH7455U = HH7455U.isnull().sum().sum()
72
73
74 nan_values_HH4117U, nan_values_HH4266U, nan_values_HH7453U,
    nan_values_HH7455U,

```

The Recharge stress is added with calculated evapotranspiration and input data of precipitation from SMHI (2025).

```

1 # Recharge
2 # Evapotranspiration

```

B. Appendix: Python code

```
3 Evap = pd.read_excel(r'C:\Line-of-path-to-file\evap.xlsx', parse_dates
  = [0], index_col=0, ).squeeze("columns")
4
5 # Precipitation [m/day]
6 Prec = pd.read_excel(r'C:\Line-of-path-to-file\prec.xlsx', parse_dates
  = [0], index_col=0).squeeze("columns")
7 # Group by every 7th day or by week
8 Evap = Evap.groupby(pd.Grouper(freq='7D')).mean()
9 Prec = Prec.groupby(pd.Grouper(freq='7D')).mean()
10
11 # Creating stresses
12 recharge_stress = ps.RechargeModel(prec=Prec, evap=Evap, rfunc=ps.Gamma
  ())

1 # Leakage and Infiltration
2
3 # Importing Leakage [m3/day]
4 Leak_raw = pd.read_excel(r'C:\Line-of-path-to-file\leakage.xlsx',
  parse_dates=[0], index_col=0)
5
6 Leak = Leak_raw.groupby(pd.Grouper(freq='7D')).mean() # Weakly data
7 Leak = Leak.fillna(Leak.mean()) # Fill NaN-values
8 Leak["Leakage"] = Leak["Leakage"].replace(0, 0.001) # Removes 0-values
9
10 # Infiltration is set to 7.2 [m3/day]
11 Infiltration = pd.DataFrame({'Dates': pd.date_range(start='2017-01-01',
  end='2024-12-31', freq='D'), 'Infiltration': 7.2})
12 Infiltration = Infiltration.set_index('Dates') # Set index to Dates
13
14 # Distances from well to stress source
15 # (longitude, latitude or X, Y)
16
17 # Coordinates for wells
18 Coord4117=[147645,6397480]
19 Coord4266=[147754,6397646]
20 Coord7453=[147667,6397579]
21 Coord7455=[147813,6397589]
22
23 obs_wells = np.array([Coord4117, Coord4266, Coord7453, Coord7455])
24
25
26 # Coordinates "Handelsschaktet" or the point of Leakage source
27 Cord_H = np.array([[147764,6397558]])
28
29
30 # Coordinates infiltration well
31 Cord_inf = np.array([[147714.5986,6397535.101]])
32
33
34 # Calculate distances matrix
35 distances_leak_H = cdist(obs_wells, Cord_H, metric='euclidean').flatten
  ()
36 distances_inf = cdist(obs_wells, Cord_inf, metric='euclidean').flatten
  ()
```

A Pastas model is created with the name "MeasuredModelHH4117U". Stesses for

Recharge is added as a stressmodel. Leakage and infiltration are also made with distance incorporated as WellModels. This segment is copied and made for all of the wells.

```

1 MeasuredModelHH4117U = ps.Model(HH4117U)
2
3 # Distances from well to stress source
4 H_HH4117U = distances_leak_H[0].item()
5 inf_HH4117U = distances_inf[0].item()
6
7 # Creating stressmodel
8 leak_stress_H_HH4117U = ps.WellModel([Leak], name="Leakage", distances
   = [H_HH4117U], rfunc=ps.HantushWellModel(), up=False, settings="well
   ")
9 inf_stress_HH4117U = ps.WellModel([Infiltration], name="Infiltration",
   distances=[inf_HH4117U], rfunc=ps.HantushWellModel(), up=True,
   settings="well")
10
11 # Adding stress models
12 MeasuredModelHH4117U.add_stressmodel(recharge_stress)           #
   Recharge stress, same stress for every borrhole Pastas model.
13 MeasuredModelHH4117U.add_stressmodel(leak_stress_H_HH4117U)   # Leakage
   "Handelsschaktet"
14 MeasuredModelHH4117U.add_stressmodel(inf_stress_HH4117U)     #
   Infiltration
15
16 # Solve and plotting
17 MeasuredModelHH4117U.solve()
18 MeasuredModelHH4117U.plots.results(tmin='2020', figsize=(12,7) )

```

B.4 Appendix: Python code for benchmark generated time series

The following section includes the code for Pastas model using MODFLOW simulated values. Both the base scenario and A, B and C shaft are described in the following code. The example shown is for when all of the shafts are added including A, B and C. Simulation for when only the Handels shaft is implemented is identical but other input data files and excluded A B and C as leakage stresses. The following code is behind the results shown in 3.3

```

1
2 # Importing packages
3 import pandas as pd
4 import pastas as ps
5 import numpy as np
6 import matplotlib.pyplot as plt
7 import math
8 from scipy import stats
9 from scipy.spatial.distance import cdist
10 import matplotlib.pyplot as plt

```

B. Appendix: Python code

Simulated MODFLOW values for groundwater data is added as one excel with Pandas series defined from it.

```
1 # Read data from an excel file
2 ModelMuse_head = pd.read_excel(r'C::Line -of -path -to -file\
   modelmuse_sim_head.xlsx', parse_dates=[0], index_col=0)
3
4 # Defines dataframes
5
6 # For reference modeling
7 ModelMuse_HH4001H = ModelMuse_head["HH4001H"].to_frame()
8 ModelMuse_HH4003H = ModelMuse_head["HH4003H"].to_frame()
9
10 # Wells included in simulation for project
11 ModelMuse_HH4117U = ModelMuse_head["HH4107U"].to_frame()
12 ModelMuse_HH4117U = ModelMuse_head["HH4117U"].to_frame()
13
14 ModelMuse_HH4266U = ModelMuse_head["HH4266U"].to_frame()
15 ModelMuse_HH4297B = ModelMuse_head["HH4297B"].to_frame()
16
17 ModelMuse_HH7453U = ModelMuse_head["HH7453U"].to_frame()
18 ModelMuse_HH7454U = ModelMuse_head["HH7454U"].to_frame()
19
20 ModelMuse_HH7455U = ModelMuse_head["HH7455U"].to_frame()
21
22 # Dataframes:
23 # ModelMuse_HH4001H, ModelMuse_HH4003H, ModelMuse_HH4117U,
24 # ModelMuse_HH4266U,
25 # ModelMuse_HH7453U, ModelMuse_HH7454U, ModelMuse_HH7455U
26
27 # Leakage [m3/day]
28 LeakLeak = pd.read_excel(r'C::Line-of-path-tofile\Leakage_sim_only_h.
   xlsx', parse_dates=[0], index_col=0)
29
30 # Defining dataframes
31 Leak_handels = LeakLeak["Leakage"].to_frame()
32 Leak_H = Leak_ABC["Handels"].to_frame()
33 Leak_A = Leak_ABC["A"].to_frame()
34 Leak_B = Leak_ABC["B"].to_frame()
35 Leak_C = Leak_ABC["C"].to_frame()
36
37
38 # Infiltration [m3/day]
39 inf = pd.read_excel(r'C:\:Line-of-path-to-file\simulated_inf.xlsx',
   parse_dates=[0], index_col=0)
40
41 # Cordinates Infiltration
42 Cord_inf = np.array([[147714.5986,6397535.101]])
43
44 # Distances Infiltration
45 distances_inf = cdist(obs_wells, Cord_inf, metric='euclidean').flatten
   ()
```

Pastas model is created using using simulated MODFLOW input data an all ABC shafts. The Leakage is added in a Matrix for the value of amount of flow and its respective distance between source and well.

```

1 # Create Pastas Model
2 # HH4117U
3
4 ModelMuse_ModelHH4117U_ABC = ps.Model(ModelMuse_HH4117U_ABC)
5 ModelMuse_ModelHH4117U_ABC.add_noisemodel(ps.ArNoiseModel())
6
7 # Distances from well to stress source
8 HH4117U_H = distances_leak_H[2].item()
9 HH4117U_A = distances_leak_A[2].item()
10 HH4117U_B = distances_leak_B[2].item()
11 HH4117U_C = distances_leak_C[2].item()
12 HH4117U_inf = distances_inf[2].item()
13 # It takes out the desired value from earlier created distance matrix.
    The matrix starts from 0 with well HH4117U being represented as a
    "2" as the third well in the column.
14
15
16 Leak_distances_HABC = [HH4117U_H, HH4117U_A, HH4117U_B, HH4117U_C]
17
18
19 # Creating stressmodel
20 leak_stress_HABC_HH4117U = ps.WellModel(Leak_HABC, name=['Handels', 'A'
    , 'B', 'C'], distances=Leak_distances_HABC, rfunc=ps.
    HantushWellModel(), up=False, settings="well")
21 inf_stress_HH4117U = ps.WellModel([inf], name="Infiltration", distances
    =[HH4117U_inf], rfunc=ps.HantushWellModel(), up=True, settings="
    well")
22
23 #Adding stress models
24 ModelMuse_ModelHH4117U_ABC.add_stressmodel(recharge_stress)
25 ModelMuse_ModelHH4117U_ABC.add_stressmodel(leak_stress_HABC_HH4117U)
26 ModelMuse_ModelHH4117U_ABC.add_stressmodel(inf_stress_HH4117U)
27
28 # Solve and plotting
29 ModelMuse_ModelHH4117U_ABC.solve()
30 ModelMuse_ModelHH4117U_ABC.plots.results()

```

Another way to model a confined aquifer with pasta is by using a lasagna model. The pasta sheets in the lasagna serve as confining layers, while the flow of béchamel sauce can be modeled through the minced meat medium.

C

Pastas models plotted graphs

The following appendix includes plotted graph of Pastas models. The wells used in the final results includes HH4266U, HH7453U and HH7455U.

C.1 Pastas, measured values

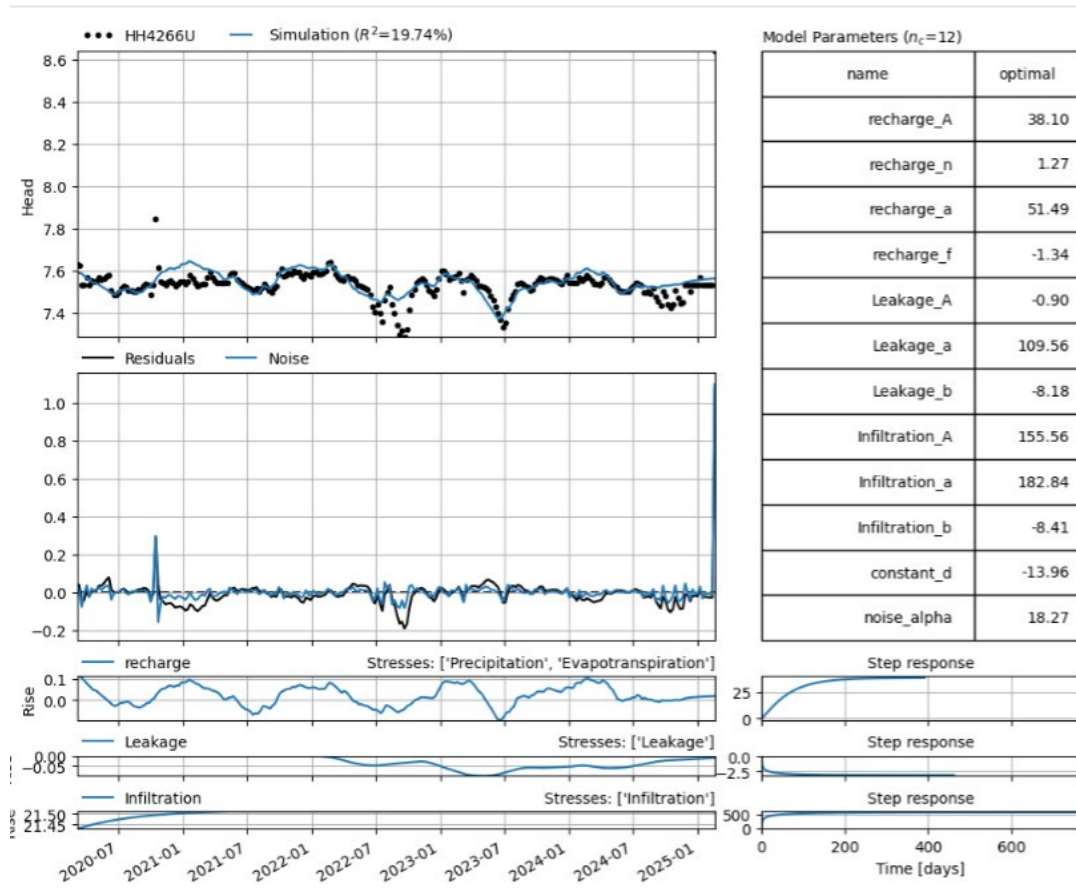


Figure C.1: Pastas simulation based on measured values for HH4266U.

C. Pastas models plotted graphs

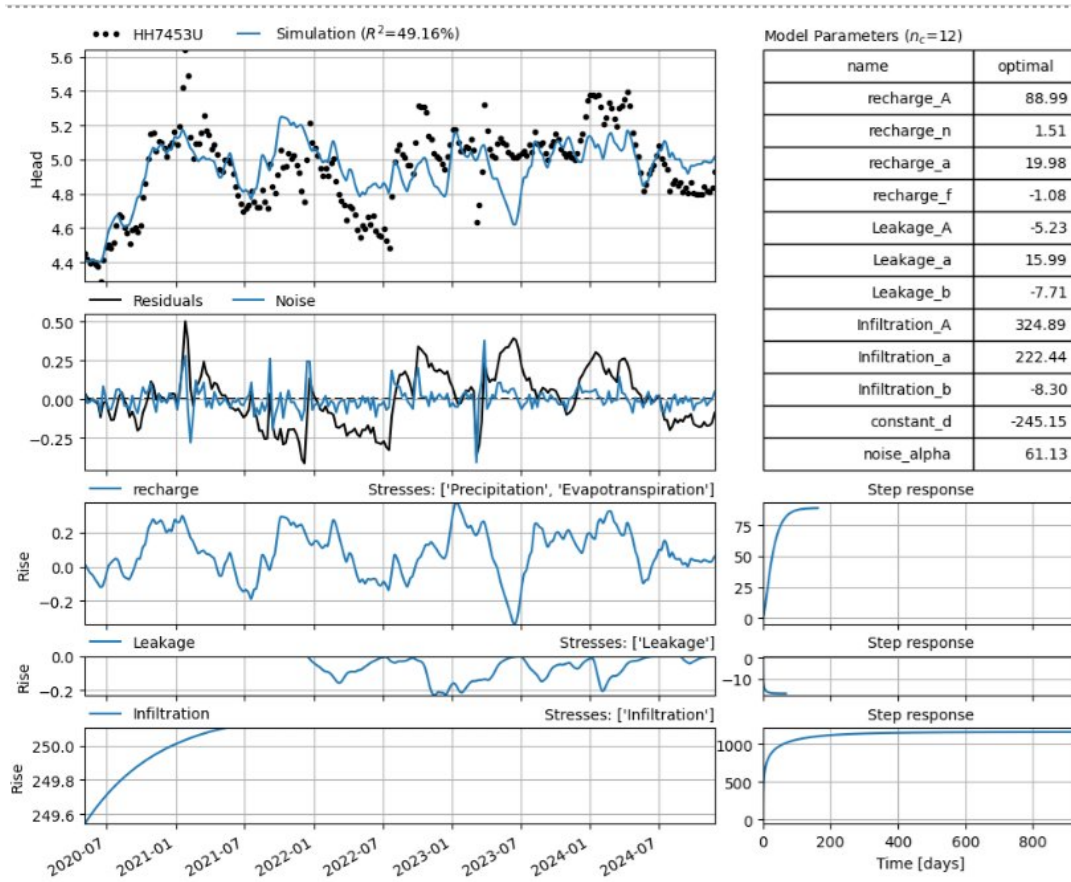


Figure C.2: Pastas simulation based on measured values for HH7453U.

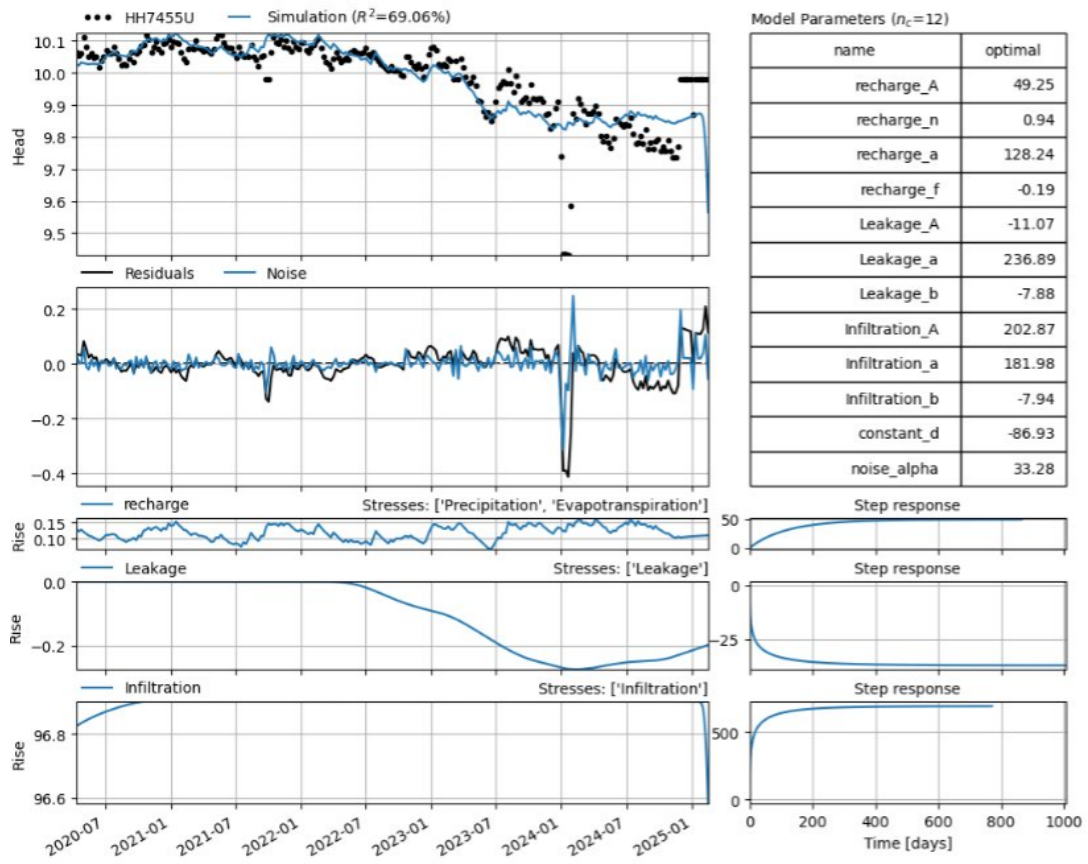


Figure C.3: Pastas simulation based on measured values for HH7455U.

C.2 Appendix: Pastas models, simulated values with constructed disturbances

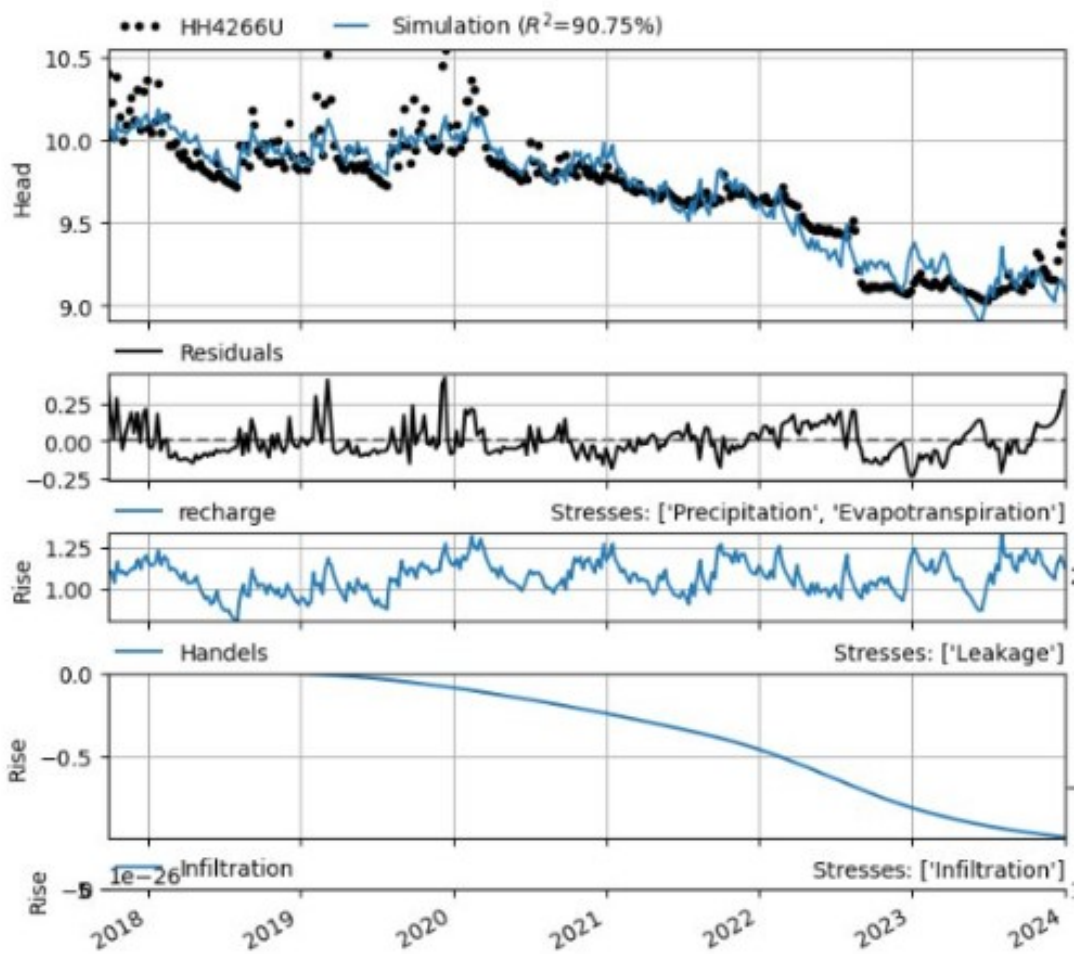


Figure C.4: Pastas simulation based on simulated values for HH4266U.

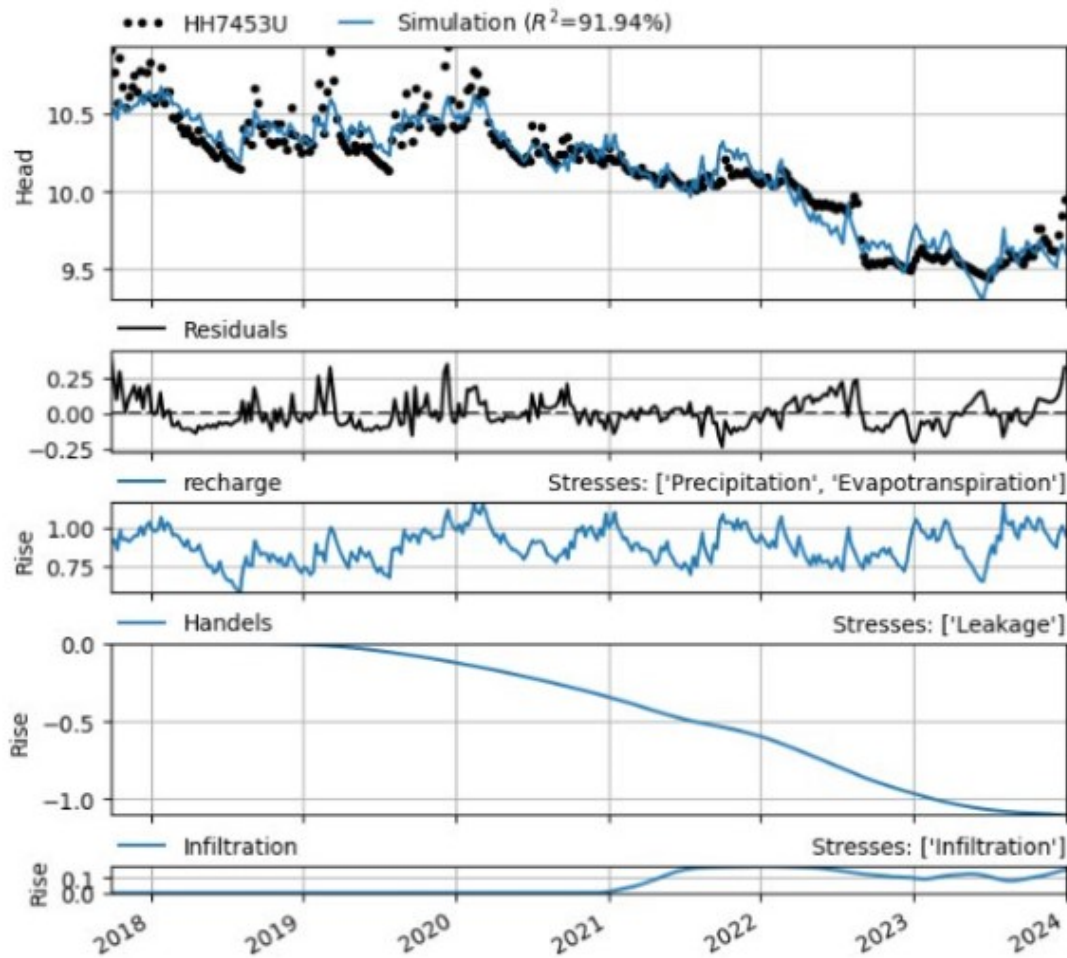


Figure C.5: Pastas simulation based on simulated values for HH7453U.

C.2.1 Estimated groundwater head with constructed disturbances

Simulated Pastas with limited time of calibration. Values from MODFLOW with the constructed disturbances have been used for the calibration.

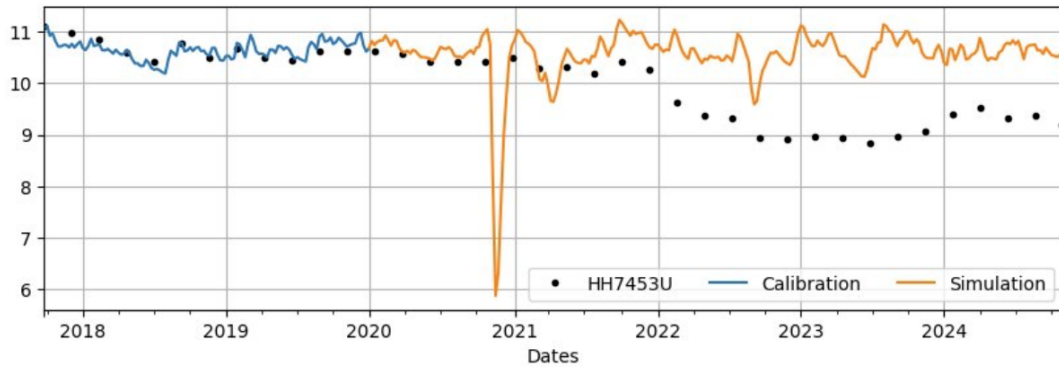


Figure C.6: Pastas simulation with limited calibration based on simulated values for HH7453U.

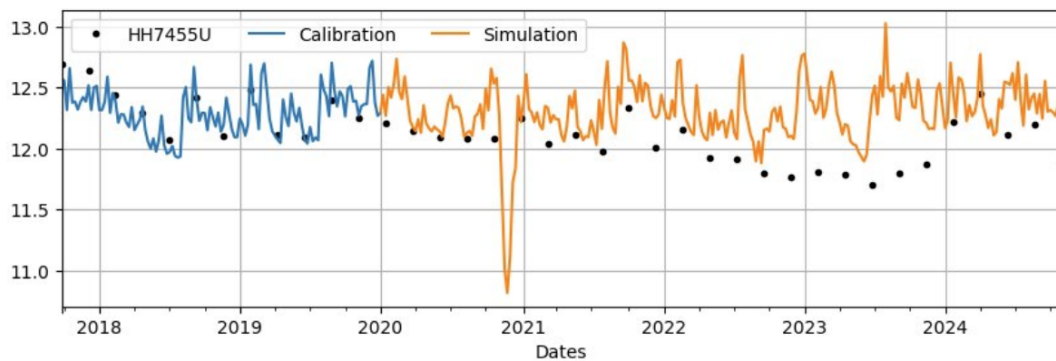


Figure C.7: Pastas simulation with limited calibration based on simulated values for HH7455U.

C.3 Appendix: Pastas models, simulated values with synthetic disturbances from A, B and C shaft

The following appendix includes Pastas simulations with all of the shafts modeled as disturbances. Shafts A, B, and C are added to the model in addition to the Handels shaft.

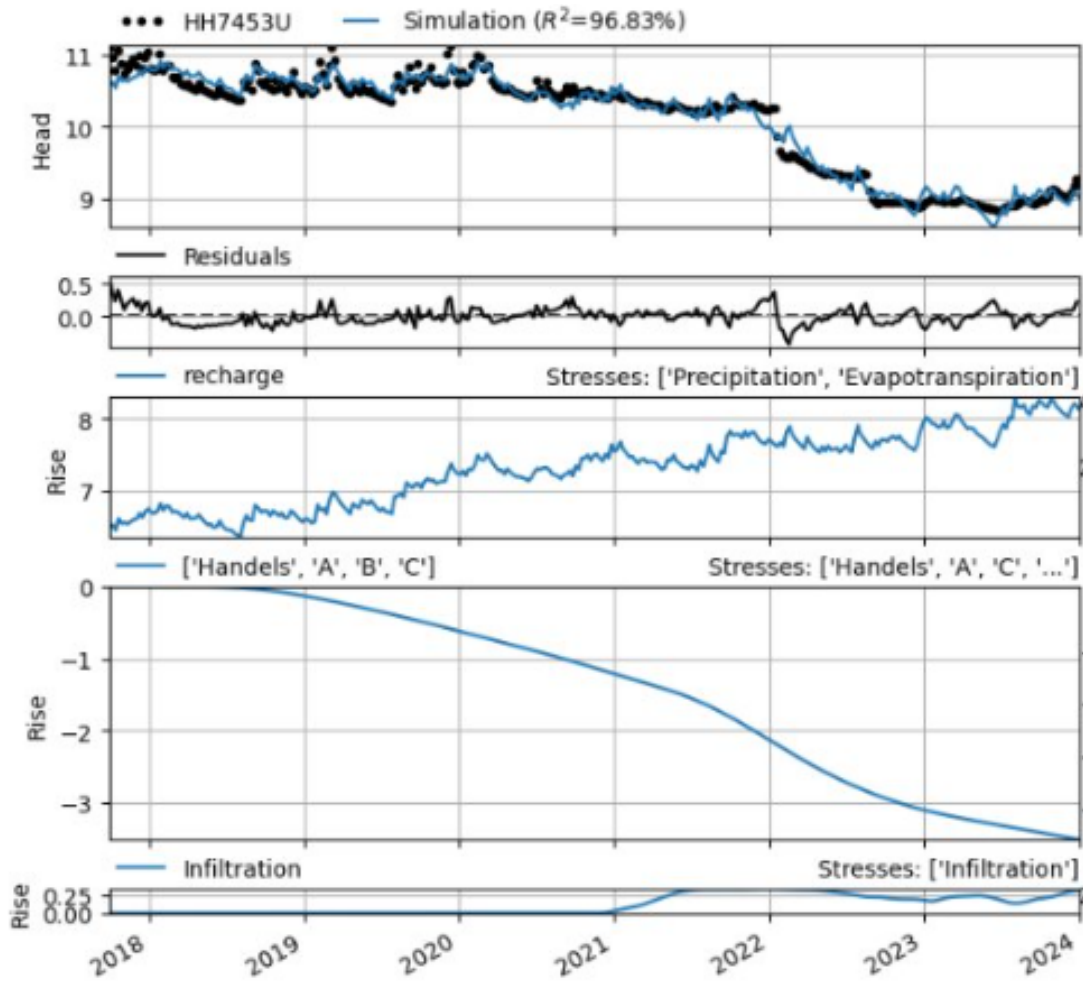


Figure C.8: Pastas simulation with shaft A, B and C on simulated values for HH7453U.

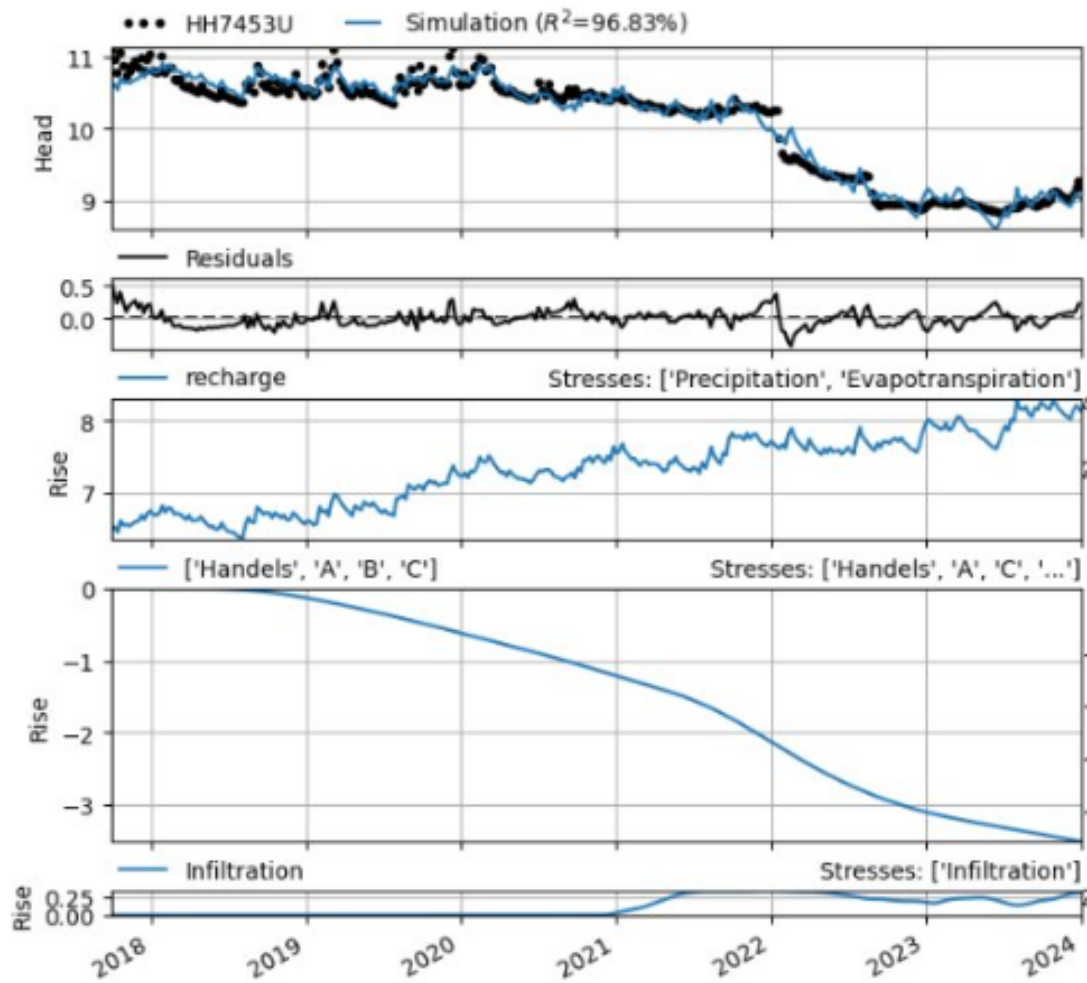


Figure C.9: Pastas simulation with shaft A, B and C on simulated values for HH7455U.

DEPARTMENT OF ARCHITECTURE AND CIVIL ENGINEERING
CHALMERS UNIVERSITY OF TECHNOLOGY
Gothenburg, Sweden
www.chalmers.se



CHALMERS
UNIVERSITY OF TECHNOLOGY